Biosensors and Bioelectronics: X 27 (2025) 100705

Contents lists available at ScienceDirect

Biosensors and Bioelectronics: X

journal homepage: www.journals.elsevier.com/biosensors-and-bioelectronics-x

Illuminating mitochondrial metabolism with genetically encoded fluorescent indicators

C. Aburto [b], A. Pinilla [b], F. Carrera-Arenas [c], A. San Martín [a,b,*]

[a] Facultad de Medicina, Universidad San Sebastián, 5110773, Valdivia, Chile
[b] Centro de Estudios Científicos (CECs), 5110466, Valdivia, Chile
[c] Facultad de Ciencias, Universidad San Sebastián, 5110773, Valdivia, Chile

A B S T R A C T

Mitochondria are recognized as dynamic metabolic hubs that integrate bioenergetic, biosynthetic and signaling functions well beyond ATP production. Their matrix hosts the Krebs cycle, fatty acid β-oxidation, and key branches of amino-acid metabolism, while also supporting heme synthesis, the urea cycle, calcium handling and redox homeostasis. Dissecting these intertwined pathways demands tools that can report metabolite dynamics *in situ*, where native ion gradients and macromolecular crowding are preserved. Genetically encoded fluorescent indicators are protein-based indicators whose spectroscopic properties shift upon binding the target metabolite. Because they are genetically encoded, these fluorescent indicators can be expressed in specific cell types and targeted to subcellular compartments, allowing real-time, non-invasive tracking of metabolic dynamics in living systems. This systematic review surveys the state-of-the-art in mitochondrial GEFIs, cataloguing fluorescent indicators for monocarboxylates, Krebs-cycle intermediates, amino acids, redox cofactors and energy nucleotides. Additionally, we outline core design principles, summarize strategies that ensure efficient targeting into the mitochondrial matrix, and discuss challenges for their correct application. By charting current capabilities and knowledge gaps, this review aims to guide the next generation of mitochondrial GEFIs and to accelerate quantitative mapping of metabolic networks at subcellular resolution.

1. Introduction

Mitochondria, often depicted as the cell's powerhouses, play a far more intricate role in cellular physiology than solely generating adenosine triphosphate (ATP) through oxidative phosphorylation (Nunnari and Suomalainen, 2012). These organelles are dynamic metabolic hubs, orchestrating a wide array of biochemical pathways critical for cellular function and survival. Key among these are the Krebs cycle, which generates reducing equivalents and biosynthetic precursors (Krebs and J, 1937), fatty acid β-oxidation (Lehninger, 1946), a major source of acetyl-CoA (Kennedy and Lehninger, 1949), and significant portions of amino acid metabolism, including both catabolism and synthesis (Braunstein and Kritzmann, 1937; Krebs and Johnson, 1980). Furthermore, mitochondria are indispensable for processes such as heme biosynthesis (Sano et al., 1959), urea cycle activity in certain tissues (Haskins et al., 2020; Helman et al., 2014), calcium homeostasis (Vasington and Murphy, 1962), maintenance of redox balance (Boveris and Chance, 1973), and the regulation of programmed cell death (Liu et al., 1996). The metabolic state within mitochondrion is not isolated; it dynamically communicates with and is influenced by the highly crowded cellular environment, positioning mitochondrion as crucial integrators and regulators of cellular status and signaling networks (Martinez-Reyes and Chandel, 2020). This interconnectedness underscores the importance of understanding mitochondrial function in the context of an intact cell where the complexity of intracellular milieu is still untouched.

To unravel the complex regulatory mechanisms governing mitochondrial function, it is essential to employ tools capable of measuring metabolite concentrations and fluxes with high spatiotemporal resolution, within the distinct microenvironments of the organelle and in real-time. Traditional biochemical approaches, which typically involve cell lysis and bulk analysis of mitochondrial extracts, obscure this vital spatiotemporal information (Chen et al., 2016). Such methods often measure total metabolite levels (bound and free) rather than the biologically active free concentrations, and they average out the heterogeneity that exists both between individual mitochondrion (MacDonald et al., 2019; Singh et al., 2023) and within different mitochondrial compartments (Hu et al., 2008), e.g., matrix and intermembrane space (IMS). Metabolism within mitochondrion is highly compartmentalized, with specific metabolite pools and enzymatic reactions localized to these

This article is part of a special issue entitled: Smart Biosensors published in Biosensors and Bioelectronics: X.

* Corresponding author. Facultad de Medicina, Universidad San Sebastián, 5110773, Valdivia, Chile.
E-mail address: alejandro.sanmartin@uss.cl (A. San Martín).

https://doi.org/10.1016/j.biosx.2025.100705
Received 1 August 2025; Received in revised form 23 September 2025; Accepted 21 October 2025
Available online 23 October 2025

distinct regions (Wang et al., 2025). For instance, the TCA cycle enzymes are predominantly in the matrix, while the electron transport chain components are embedded in the internal mitochondrial membrane. Consequently, understanding the precise localization and dynamics of metabolites within these sub-compartments is critical for a complete picture of mitochondrial function. The progression from test tube biochemical assays employing isolated mitochondria to the use of fluorescent dyes, which improved live-cell imaging but often lacked specificity and true subcellular targeting. Fluorescent tools based on proteinaceous reporters represent a significant advancement in this pursuit, enabling researchers to probe mitochondrial function with unprecedented detail within the native cellular context.

Genetically encoded fluorescent indicators (GEFIs) are chimeric proteins engineered from a ligand-binding moiety fused to fluorescent protein(s) (FPs) reporters, that dynamically monitored the concentration and metabolic fluxes of specific analytes through alterations in their optical properties (Frei et al., 2024). A key advantage of GEFIs is their genetic encodability, which allows for their expression in living cells, tissues, and even whole organisms through standard gene delivery techniques. This property enables their precise targeting to specific subcellular compartments such as mitochondria, by fusing them with appropriate mitochondrial targeting sequences (MTS). Compared to older methods like the microinjection of synthetic dyes, GEFIs offer relatively low invasiveness and permit chronic monitoring of metabolic changes in defined cell types or specific mitochondrial populations over extended periods. This capability is fundamental for studying dynamic processes in both time and space, allowing for the investigation of how specific mitochondrial metabolite pools respond to various physiological stimuli, pharmacological interventions, or pathological conditions *in situ* and in real time.

Key metabolites, such as ATP, NADH, and pyruvate, exist in distinct pools in both the cytosol and mitochondria (Arce-Molina et al., 2020; Hu et al., 2021; Imamura et al., 2009), often at different concentrations and subject to independent regulation and roles. Measurements of whole-cell or cytosolic levels of these metabolites can therefore provide an incomplete or even misleading picture of the specific metabolic activities occurring within mitochondria. Mitochondrially-targeted GEFIs emerge as an indispensable tool for distinguishing the unique contributions and regulation of mitochondrial metabolic pathways from those in other cellular compartments.

This systematic review aims to provide a comprehensive overview of the current landscape of GEFIs that have been specifically designed and successfully targeted to mitochondria for the real-time detection of key classes of metabolites. The metabolite categories covered include monocarboxylates, Krebs cycle intermediates, amino acids, redox cofactors and energy nucleotides. We will delve into the fundamental design principles and sensing mechanisms of these mitochondrial GEFIs and discuss the strategies employed for their effective targeting to the mitochondrial matrix. Furthermore, it will highlight significant applications and key findings derived from the use of these sophisticated tools in unraveling the complexities of mitochondrial metabolic dynamics. A critical evaluation of the advantages, inherent limitations, and ongoing challenges associated with these sensors will be provided, alongside an identification of existing gaps in the current GEFI toolkit for mitochondrial research.

2. Mitochondrial metabolism

Mitochondria are the final destination for the catabolism of the three major classes of energy-rich macromolecules: carbohydrates, fats, and proteins. While glycolysis, the initial breakdown of glucose, occurs in the cytosol, the complete oxidation of its product, pyruvate, as well as the oxidation of fatty acids and amino acids, takes place within the mitochondrial matrix. These pathways converge on the production of acetyl-CoA and other key intermediates that fuel the tricarboxylic acid (TCA) cycle, the central engine of cellular respiration (Nunnari and Suomalainen, 2012). The reducing equivalents generated from these oxidative processes, in the form of NADH and FADH2, subsequently donate their high-energy electrons to the electron transport chain, driving the synthesis of ATP. This process links the cytosolic glycolytic pathway with the TCA cycle and oxidative phosphorylation, ensuring an efficient conversion of glucose into ATP.

Carbohydrate-derived energy into the mitochondria begins with pyruvate, the end product of glycolysis. Because the enzymes for its complete oxidation are located within the mitochondrial matrix, where pyruvate is positioned at a key metabolic crossroads. Before it can enter the central TCA cycle, it must be converted into acetyl-CoA. This conversion is an irreversible reaction known as oxidative decarboxylation, catalyzed by the pyruvate dehydrogenase complex (Patel and Korotchkina, 2006). During this process, NAD^+ is reduced to NADH, capturing high-energy electrons that will later be used for ATP production.

Pyruvate is not the only molecule that can feed the TCA cycle. Alternatively, the proton-motive force can be maintained to produce ATP by the β-oxidation pathway adapted to handle the oxidation of fatty acids proceeds through the normal β-oxidation spiral until the final three carbons remain as propionyl-CoA. This three-carbon molecule cannot be further oxidized by the pathway. Instead, it is converted in a separate three-step, ATP-dependent process into succinyl-CoA, an intermediate of the TCA cycle. This conversion provides a direct anaplerotic entry point into the TCA cycle, replenishing its intermediates. Additional carbon source to replenish the TCA cycle intermediates is amino acids metabolism. Mitochondrial amino acid metabolism extends beyond simple energy generation; it is a dynamic, bidirectional process crucial for maintaining the balance of central metabolic pathways. The entry of amino acid-derived carbon skeletons into the TCA cycle serves as an anaplerotic function. As a prime example, we have the conversion of glutamate to α-ketoglutarate reaction catalyzed by the enzyme glutamate dehydrogenase. These reactions replenish TCA cycle intermediates that may have been withdrawn for biosynthetic purposes, ensuring that the cycle's concentration of intermediates remains stable and its oxidative flux can continue. Conversely, mitochondria are also a biosynthetic hub, providing the precursors needed for the synthesis of non-essential amino acids. This withdrawal of intermediates from the TCA cycle is known as cataplerosis. For example, mitochondrial oxaloacetate is the direct precursor for the synthesis of aspartate and asparagine, while α-ketoglutarate is the precursor for glutamate, glutamine, proline, and arginine. This bidirectional flow establishes the TCA cycle as a critical metabolic integrator, constantly balancing the cell's catabolic needs for energy with its anabolic needs for biosynthetic building blocks (Owen et al., 2002).

In addition to their central role in the catabolism of canonical fuels, mitochondria are the exclusive or partial sites of several highly specialized metabolic pathways that are essential for systemic homeostasis and the synthesis of vital cofactors. These processes, including the initial steps of nitrogen disposal via the urea cycle, the production of alternative fuels through ketogenesis, and the intricate synthesis of heme, further illustrate the principle of metabolic compartmentalization (McBride et al., 2006). By housing key steps of these pathways, the mitochondria can sequester toxic intermediates, link biosynthetic output directly to the cell's energy status, and manage the flow of metabolites between different cellular compartments. A disruption in the TCA cycle or in oxidative phosphorylation not just induced cell energy crisis but also a biosynthetic failure. For example, inhibition of the mitochondrial respiratory chain can impair the regeneration of NAD^+, which is required for the oxidation of α-ketoglutarate and malate in the TCA cycle. This can lead to a functional inhibition of the cycle, which in turn blocks the synthesis of key amino acids like aspartate, thereby halting cell proliferation (Birsoy et al., 2015; Sullivan et al., 2015). This deep interconnection explains the complex and severe phenotypes observed in mitochondrial diseases, which often involve not just energy deficiency but also profound disturbances in cellular growth and

development. Therefore, new technology is required to observe these highly dynamic metabolic processes in living cell at sub-cellular resolution.

3. Architectures and sensing mechanisms of GEFIs

Intramolecular fluorescence-based indicators report metabolic processes through an easy to detect readout. Several design strategies have been successfully employed to create GEFIs for metabolites, each with its own architecture and modalities of readouts. Intramolecular fluorescent indicators can be based on one or two fluorescent reporters (Fig. 1). This structural characteristic can affect the structural complexity and size of the indicator, which are within the main challenges for efficient mitochondrial targeting. Based on the GEFIs basic architectures they can be organized in FRET and single-fluorophore-based fluorescent indicators.

3.1. Donor/acceptor FRET-based indicators

Förster Resonance Energy Transfer (FRET)-based indicator are a widely used class of GEFIs that typically incorporate two distinct FPs, a donor (e.g. mTFP or cerulean) and an acceptor (e.g., Venus or citrine), flanking or integrating with the sensing domain (Miyawaki et al., 1997). FRET is a non-radiative energy transfer process that occurs when the donor and acceptor FPs are in close proximity (typically <10 nm) and their dipoles are favorably oriented, and when the donor's emission spectrum overlaps with the acceptor's excitation spectrum (Day et al., 2008). The interaction of the metabolite with the ligand binding moiety induces a conformational change that alters the distance or orientation between the donor and acceptor FPs, thereby modulating FRET efficiency. This change is typically measured as a ratiometric signal, the ratio of acceptor emission to donor emission upon excitation of the donor. This ratiometric output provides an inherently less sensitive to variations in sensor concentration, photobleaching rates of individual FPs, cell path length, and excitation intensity fluctuations. However, this type of GEFIs often displays low dynamic range, occupies larger spectral bandwidth precluding multiplexing measurements, and they are structurally complex and bulky making them difficult to efficiently target to mitochondria. Although the challenges associated with mitochondrial targeting of FRET-based indicators, successful cases have been reported.

FRET-based ATP biosensor called Mit-ATeam provides a highly sensitive, real-time measurement of ATP relative levels directly within the mitochondrial matrix. This precise view allowed researchers to discover that the hypoxia-inducible protein G0/G1 switch gene 2 (G0s2) positively regulates OXPHOS by interacting with the FoF1-ATP synthase complex, thereby increasing the rate of ATP production and protecting cells from hypoxic stress (Kioka et al., 2014). Another example is the ability to track pyruvate directly within the mitochondrial matrix using a targeted pyruvate fluorescent indicator Pyronic, which provide evidence needed to redefine the role of lactate in mitochondrial metabolism. Specifically, by monitoring intramitochondrial pyruvate, the fluorescent indicator allowed to show that when pyruvate entered the matrix, it was actively converted into lactate, a phenomenon that pointed to the existence of mitochondrial lactate dehydrogenase (mLDH) activity. Without the ability to precisely measure the pyruvate flux within the organelle and link it to lactate generation, it would have been difficult to prove that this conversion was happening locally. Therefore, the mitochondrially-targeted fluorescent indicator was essential for demonstrating that lactate production is an intrinsic mitochondrial process, leading directly to the proposal of the "lactate-carried energy overflow" model (Rauseo et al., 2024).

Both the Mit-ATeam and Pyronic indicators utilize the mitochondrial targeting signal from cytochrome *c* oxidase subunit VIII (COX8) to be imported to the mitochondrial matrix. A key difference in their constructs, however, is the number of targeting repeats employed: Mit-

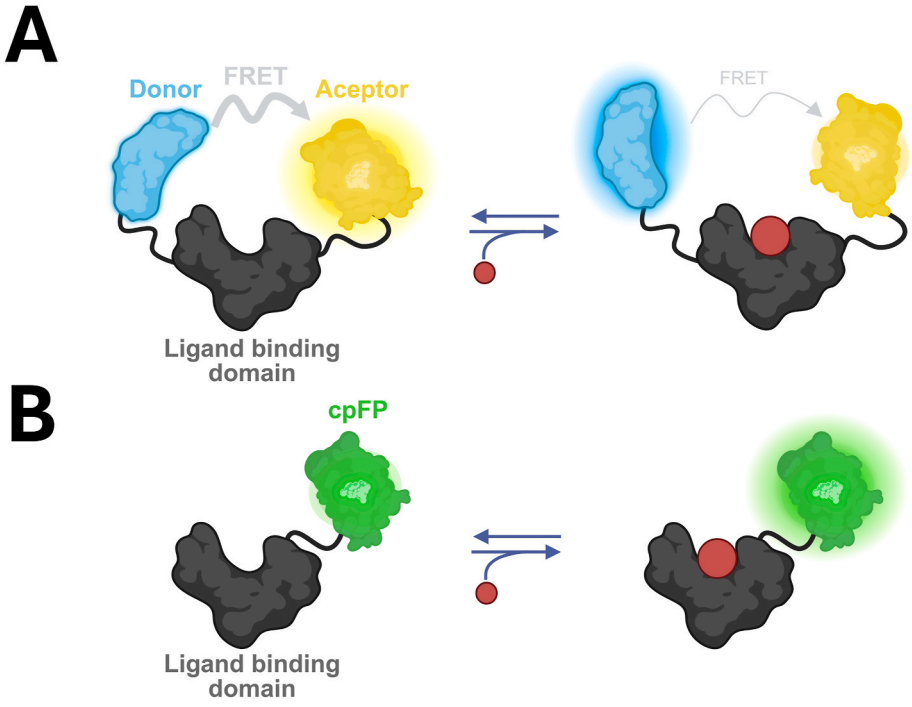

Fig. 1. Architectures of genetically encoded fluorescent indicators (GEFIs).
A) FRET-based sensors. A ligand-binding domain (LBD) is flanked between donor and acceptor fluorescent proteins whose excitation and emission spectra partially overlap. Excitation of the donor triggers non-radiative Förster energy (gray curved arrow) transfer to the acceptor by resonance to the acceptor, and ligand-induced (red circle) conformational changes in the ligand binding domain tune the efficiency of this transfer (gray curved arrows). **B)** Single-fluorophore sensors. Here, the ligand binding domain is fused directly to a circularly permuted fluorescent protein (cpFP). Binding the target metabolite (red circle) alters the chromophore's environment, thereby modulating the emitted fluorescence intensity. (For interpretation of the references to colour in this figure legend, the reader is referred to the Web version of this article.)

ATeam uses two repeats, whereas Pyronic require four. The need for additional repeats for Pyronic is attributed to its greater structural complexity. Its ligand-binding domain is the full-length bacterial transcription factor PdhR, which is composed of DNA and ligand-binding domains, making the sensor larger and more complex than the single epsilon (ε) subunit of ATP synthase used in ATeam. Consequently, using an insufficient number of COX8 repeats for the Pyronic indicator can result in incomplete mitochondrial targeting, leading to cytosolic leakage that interferes with the primary signal and prevents accurate data interpretation.

3.2. Single-fluorophore based indicators

Intensiometric sensors rely on a change in the fluorescence intensity of a single FP upon metabolite binding. A common strategy involves the use of a circularly permuted FP (cpFP), where the original N- and C-termini are joined by a peptide linker, and new termini are created near the chromophore. This circular permutation can render the FP's chromophore environment more sensitive to conformational changes in an inserted or fused sensing domain (Baird et al., 1999). The metabolite-induced conformational change in the sensing domain alters the local environment of the cpFP's chromophore, affecting its protonation state, excited-state proton transfer, or non-radiative decay pathways, leading to a change in fluorescence intensity (Akerboom et al., 2009). Single FP sensors can sometimes achieve large dynamic range and are simpler in terms of genetic construct size compared to FRET-based indicators. However, simple intensiometric readouts are susceptible to variations in sensor expression levels, photobleaching, and cell volume changes, which can complicate quantitative measurements and data interpretation.

To address the limitations intensiometric indicators can be also utilized as a ratiometric tools using a double excitation peaks subject to be modulated by the ligand binding, normalized the signal by an isosbestic point in the excitation spectrum, co-expressing a second fluorescent protein inert for the analyte of interest or fusing a second inert fluorescent protein. Double excitation peaks laid on chromophore properties, which can exist in two different, interconvertible chemical states: a protonated (neutral) form and a deprotonated (anionic) form. These two states possess distinct light absorption properties sensitive to the ligands of interest. The protonated state is responsible for the excitation peak around 440 nm, while the deprotonated state absorbs light around 488 nm. This is the case for iNap3, a GEFI for NADPH that functions ratiometrically due to its two excitation peaks (Tao et al., 2017). Upon binding NADPH, its fluorescence intensity increases when excited at ~420 nm while simultaneously decreasing upon excitation at ~485 nm, providing a large dynamic range for sensitive measurements. This property was crucial for quantifying NADPH in specific organelles. The authors created a version of the fluorescent indicator suitable to be targeted to mitochondrial, iNap3-Mit. By using this targeted GEFI, they were able to measure the NADPH concentration specifically within the mitochondrial matrix. This revealed a concentration of approximately 37 μM, which is substantially higher than the ~3 μM measured in the cytosol (Tao et al., 2017).

An isosbestic point in the excitation spectrum is also a good alternative to convert intensiometric to ratiometric readout. When measuring the ATP:ADP ratio specifically within mitochondria using PercevalHR, its isosbestic point at 440 nm was exceptionally useful (Tantama et al., 2013). Mitochondria are highly dynamic, and their constant movement and shape changes can create signal fluctuations that mimic real results. Exciting the sensor at its isosbestic point provides a control signal that is insensitive to movement-based artifacts, ensuring the final measurement reflects the true mitochondrial energy state, not just the organelle's dynamic behavior.

Co-expressing an inert second fluorescent protein with the single-fluorophore indicator is another possible approach, but it comes with the trade-off of increased the pressure to the mitochondrial import machinery, making the targeting to the mitochondria more difficult and potentially displaced native mitochondrial imported proteins. For instance, the pyruvate GEFI PyronicSF can be targeted to mitochondria and used with a co-expressed mito-mCherry as a normalizer. Using this strategy, a study produced key quantitative results on mitochondrial pyruvate metabolism (Arce-Molina et al., 2020). The primary finding was that the steady-state pyruvate concentration in astrocyte mitochondria is low, approximately 21 μM, which is lower than the level in the cytosol (33 μM). This validated approach also enabled the direct measurement of mitochondrial pyruvate consumption, with a median rate of 1.1 μM/s. Furthermore, the sensor revealed metabolic heterogeneity, demonstrating that pyruvate concentration and consumption rates can vary between different mitochondrial populations within a single cell (Arce-Molina et al., 2020).

Another approach is Matryoshka fluorescent indicator platform developed to overcome the limitations by creating a ratiometric indicator from a single-fluorophore with a large dynamic range, using as a normalizer a second fused fluorescent protein inert to the analyte of interest (Ast et al., 2017). This technology uses a single cassette called GO-Matryoshka that nests a stable reference FP, the large Stokes shift LSSmOrange inside a reporter FP, a circularly permuted green FP (cpEGFP). The Matryoshka biosensor platform was developed to overcome the intrinsic limitations of intensiometric reporters by creating a ratiometric indicator with a large dynamic range. This unique structure allows a single blue excitation wavelength (~440 nm) to elicit both green fluorescence from the reporter and orange fluorescence from the stable reference. As the reporter's green fluorescence changes in response to an analyte, the orange reference signal remains largely stable, providing a ratiometric readout. This intrinsic normalization corrects for expression and instrumental artifacts, allowing for improved quantitation while retaining the desirable high dynamic range of single-FP sensors.

4. Mitochondrial targeting of GEFIs

The modular nature of the MTS has been widely exploited in molecular biology to direct a vast array of proteins to the mitochondrial matrix. The most common and well-characterized mechanism for directing proteins to the mitochondrial matrix relies on a cleavable N-terminal pre-sequence, also known as a mitochondrial targeting sequence. This pathway is the most frequently exploited for targeting GEFIs to the matrix, providing a robust method for visualizing mitochondrial morphology, dynamics, and distribution in living cells. This N-terminal pre-sequences are cleavable sequences, usually 15–50 amino acids in length, although variations exist. They are characterized by an abundance of positively charged (arginine, lysine) and hydrophobic amino acids, and they have a propensity to form an amphipathic α-helix, structure is recognized by the mitochondrial import machinery (Gavel et al., 1988; von Heijne, 1986).

COX8 or COXVIII: The pre-sequence from subunit VIII of cytochrome *c* oxidase (MSVLTPLLLRGLTGSARRLPVPRAK) is one of the most widely used and effective MTS for targeting exogenous proteins, including GEFIs, to the mitochondrial matrix in mammalian cells. To enhance import efficiency, particularly for large or complex fusion proteins like many GEFIs, tandem repeats of the COX8, e.g., 2xCOX8 or 4xCOX8 are often employed (Rizzuto et al., 1995; Tkatch et al., 2017).

To investigate mitochondrial glutamine, the single-fluorophore GEFI Mito-GlutaR was fused into four copies of the COX8 mitochondrial targeting sequence to the N-terminus of the GlutaR indicator (Liu et al., 2025). This strategy effectively localized the fluorescent indicator within the mitochondrial matrix, enabling a key result through specific measurement of the organelle's glutamine pool. The targeted approach revealed that the free glutamine concentration in mitochondria is approximately 160 μM, which is significantly lower than the level in the cytosol. This quantitative comparison supports the conclusion that mitochondria are a primary site of glutamine consumption in the cell

(Liu et al., 2025)

Subunit 9 of F1Fo-ATPase (Su9): Another well-established and commonly used MTS is derived from the N-terminal region (MALSRAVSLRASLRVLSASRIRLSPAAQALRRSSTSL) of subunit 9 of the F1Fo-ATPase from *Neurospora crassa* (Galanis et al., 1991; Rojo et al., 1995; van den Boogaart et al., 1982). This sequence has also proven effective for targeting various proteins to the mitochondrial matrix in diverse eukaryotic systems.

The lactate single-fluorophore GEFI FiLa-Mit was mitochondria targeted by fusing a signal sequence from *Neurospora crassa* ATP synthase to the N-terminus. This strategy successfully localized the fluorescent indicator to the mitochondrial matrix, enabling direct and specific measurements of the lactate pool within the organelle (Li et al., 2023).

There are alternative MTS that can potentially be useful to target GEFIs to mitochondrial matrix. For instance, the Ornithine Transcarbamylase that is found in the human Ornithine Transcarbamylase, a key enzyme in the urea cycle (MLFNLRILLNNAAFRNGHNFMVRNFRCGQPLQ) (Horwich et al., 1986; Kanazawa et al., 1997). The MTS from mitochondrial isoform of Superoxide Dismutase 2, also known as MnSOD a critical antioxidant enzyme in the matrix, is another good alternative to target GEFIs to mitochondrial matrix (MLSRAVCGTSRQLAPVLGYLGSRQKHSL) (Kong et al., 2003). Pyruvate Dehydrogenase E1α Subunit (PDHA1); the leader sequence of the E1α subunit of the pyruvate dehydrogenase complex is another well-established alternative to drive proteins towards mitochondria (MRLTAARALLPRVLCARARASTSVPRSRA) (Ho et al., 1989; Owen et al., 2000).

Successful mitochondrial protein targeting is a complex process that extends beyond the mere selection of a MTS. The import efficiency is critically influenced not just by the MTS, but also by the targeted protein that can dramatically alter the outcome (Eilers et al., 1988; Vestweber and Schatz, 1988; Wiedemann and Pfanner, 2017). Since precursor proteins must be unfolded to pass through import channels, a targeted protein that is very stable or folds too rapidly can stall translocation, leading to its degradation or aggregation and triggering cellular proteotoxic stress. Furthermore, MTSs possess a spectrum of potencies, from "strong" to "weak". While a strong MTS like the commonly used COX8A can be highly effective, its overuse at high expression levels can saturate the import machinery. This creates a stagnation of targeted proteins at the mitochondrial surface, competitively inhibiting the import of essential endogenous proteins and causing mitochondrial dysfunction. In this scenario, the reporter protein ceases to be a passive observer and becomes an active perturbing agent, confounding experimental results and highlighting the need for a diverse toolkit of MTSs with varying strengths to ensure experimental accuracy.

4.1. Considerations for targeting efficiency and compartment specificity

Achieving the proper localization and concentration of a GEFI within the mitochondrial matrix requires a careful balance between several factors. This includes the expression level and structural characteristics of the GEFI, the potency of the MTS, and the number and position of tandem MTS repeats. The primary goal is to deliver a sufficient amount of the fluorescent indicator to the mitochondrial matrix to achieve an optimal signal-to-noise ratio for detecting signals from a single mitochondrion. However, this must be accomplished without overwhelming the mitochondrial import machinery, which is essential for importing endogenous proteins, or causing significant "leakage" of the indicator into the cytosol. An excessive cytosolic signal can contaminate measurements and obscure the interpretation of results.

The difficulty in striking this balance is highly dependent on the gene delivery system used. For instance, transient transfection with plasmids often leads to high variability in copy number delivered and expression levels, making it difficult to control the amount of protein produced and thus increasing the risk of cytosolic leakage. In contrast, viral transduction systems, such as those using lentiviruses or adeno-associated viruses, offer better control as they typically result in a more limited and stable number of gene copies integrated into the host genome. For *in vivo* experiments, knock-in models, where the GEFI is inserted into a specific genomic locus, represent the gold standard. In this scenario, expression is controlled by endogenous regulatory elements, leading to more physiologically relevant protein levels (Arce-Molina et al., 2020). Therefore, combining a tightly controlled expression system with a potent MTS is a robust strategy. The need for tandem MTS repeats often depends on the size and structural complexity of the GEFI. Indicators based on FRET, which are often larger multi-protein constructs, may require multiple MTS repeats for efficient mitochondrial import. In contrast, single-fluorophore indicators are typically smaller and can often be targeted effectively with a single MTS. However, there are exceptions. For example, ATeam, a FRET-based ATP indicator, and Lapronic, a lactate/pyruvate ratio indicator, are efficiently targeted to mitochondria using a single MTS, despite being engineered on three protein moieties (Galaz et al., 2020; Imamura et al., 2009). The key point is the use of relatively small bacterial binding proteins to build these fluorescent indicators. It is also crucial to consider that excessive MTS repeats can sometimes interfere with the indicator's function or folding. Consequently, it is advisable to use the minimum number of MTS repeats necessary for effective targeting. To validate a signal's origin functional protocols that elicit a predictable, compartment-specific response from the GEFI could be useful. This approach involves applying a specific stimulus known to primarily affect the mitochondrial environment. The key is that the GEFI population within the mitochondria will respond differently and predictably compared to any contaminating GEFI population in the cytosol (Arce-Molina et al., 2020; Imamura et al., 2009). Additionally, the co-localization with mitochondrial markers or the use of membrane-potential-sensitive dyes could help to assess how much of the GEFI signal as a mitochondrial origin.

5. Mitochondria-targeted GEFIs for metabolites

Since the inception of the first GEFI for an organic molecule (Fehr et al., 2002), over 20 different metabolites can now be monitored using this technology. This collection includes more than 50 distinct GEFIs (San Martin et al., 2022), ranging from high-performance indicators to first-generation prototypes suitable for a variety of experimental scenarios. The majority of the current GEFIs for metabolite have been optimized for the cytosol, enabling measurements with single-cell resolution. However, as these fluorescent indicators are genetically encodable tools, they possess the potential to achieve sub-cellular resolution. Currently, just a small number of these GEFIs have been tested for functionality within the mitochondrial matrix (Fig. 2). This technological gap hampers the assessment of mitochondrial metabolism and its regulatory nuances in a comprehensive manner, while preserving the complexity of the intracellular and sub-cellular milieu. To present a comprehensive picture of the state-of-the-art of mitochondrially targeted GEFIs, we have surveyed the literature to provide to our readers with an overview of the available fluorescent indicators to probe mitochondrial metabolism and the key features required for their used them within this fascinating organelle.

5.1. Monocarboxylate indicators

Monocarboxylates are small, organic molecules structurally defined by a single carboxylate group, making them vital, water-soluble carriers of energy and carbon. Metabolically, they are central intermediates that link major energy-producing pathways, such as the breakdown of sugars and fats, with the mitochondrial tricarboxylic acid cycle. Their importance lies in their ability to shuttle energy between different cells and tissues, ensuring metabolic flexibility in response to varying physiological demands (Brooks, 1986, 2018; Juel and Halestrap, 1999). For instance, the end-product of glycolysis pyruvate can either enter

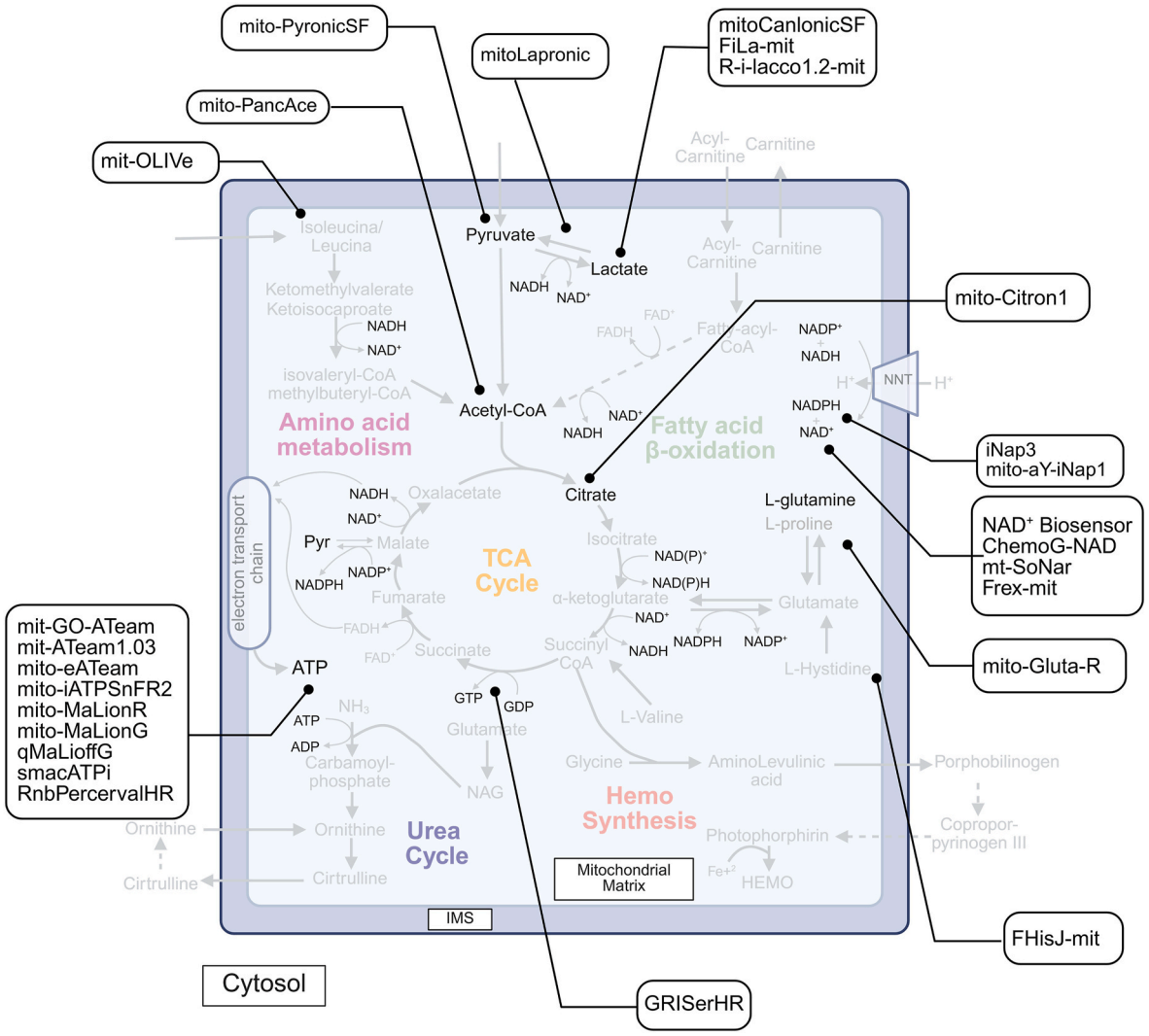

Fig. 2. Schematical overview of mitochondrial metabolism and the available mitochondria-targeted GEFIs. Major pathways operating in mitochondria: TCA cycle, amino-acid metabolism, fatty-acid β-oxidation, the urea cycle, and heme biosynthesis; together with key redox transformations that sustain bioenergetics and redox homeostasis (NAD^+/NADH, $NADP^+$/NADPH, FAD/$FADH_2$) and the nicotinamide-nucleotide transhydrogenase (NNT). Metabolites in black denote targets for which mitochondria-targeted GEFIs are available, while metabolites in gray denote metabolic points where GEFIs have not been developed. Solid arrows denote established steps; dotted arrows indicate multiple steps for simplicity. IMS, intermembrane space; NAG, N-acetylglutamate; NNT, nicotinamide nucleotide transhydrogenase. Created in BioRender. https://BioRender.com/mf6f223.

mitochondria for full oxidation (Bricker et al., 2012; Herzig et al., 2012) or be converted to lactate that is shuttled between cells as a fuel source and signaling molecule (Brooks, 1986; Hui et al., 2017).

Monocarboxylates like lactate and pyruvate are suitable to be monitored within the mitochondria of intact cells using GEFIs, providing unprecedented spatiotemporal resolution. Fluorescent indicators such as FiLa (Li et al., 2023), CanlonicSF (Aburto et al., 2022; Rauseo et al., 2024), and R-iLACCO1.2 (Nasu et al., 2023) have been successfully targeted to the mitochondrial matrix, enabling direct visualization and quantification of the lactate pool. This has led to the key discovery that lactate is highly enriched in mitochondria at concentrations significantly higher than in the cytosol. Conversely, the pyruvate sensor PyronicSF revealed that mitochondrial pyruvate is maintained at a very low micromolar concentration, establishing the mitochondrial pyruvate carrier as a key regulator of metabolism. Together, these tools allow researchers to track the real-time flux of critical metabolites in living cells, defining the metabolic landscape of these vital organelles. For a comprehensive view about the features of state-of-the-art of GEFIs for monocarboxylates that have been targeted at mitochondrial matrix and their users, see Table 1.

5.2. *Krebs cycle metabolite indicators*

Krebs cycle, or tricarboxylic acid (TCA) cycle, is the central hub of cellular respiration, occurring in the mitochondrial matrix. It is a series of eight enzyme-catalyzed reactions that completely oxidizes acetyl-CoA derived from carbohydrates, fats, and proteins, into carbon dioxide. As the first molecule formed in the Krebs cycle, citrate initiates the process that links nutrient oxidation to energy production.

Currently two sensors for Krebs cycle metabolites have been successfully targeted to mitochondria. PancACe (Smith et al., 2024) and Citron1 (Zhao et al., 2020) have enabled the first real-time monitoring of acetyl-CoA and citrate, respectively. Revealing distinct dynamics of acetyl-CoA and citrate pools. However, the recent development of these first-generation tools highlights that we are in the early stages of this exploration. Indeed, just a small fraction of the Krebs Cycle metabolite can be probed using GEFIs. This hampers the ability to directly visualize the central hubs of cellular energy in real-time in the mitochondrial matrix. For a comprehensive view about the features of state-of-the-art of GEFIs for Krebs cycle metabolites that have been targeted to mitochondrial matrix and their users, see Table 2.

Table 1
Monocarboxylates fluorescent indicators tested in mammalian systems.

INDICATOR	YEAR OF PUBLICATION	LIGAND BINDING MOIETY	READOUT	MITO TARGET	*IN VITRO* K_D	ΔF or ΔR_{MAX} (%) [a]	ADDGENE NUMBER	USERS
MONOCARBOXYLATES								
LACTATE								
Mito-Canlonic	2024 (Rauseo et al., 2024)	TTHA0766	Intensiometric (cpGFP) 488	1x COX8	293 μM	80 %	224465	NA
FiLa-mit	2023 (Li et al., 2023)	LldR	Ratiometric (cpYFP) 485/420	1xSu9	130 μM	50 %	NA	NA
R-iLACCO1.2	2023 (Nasu et al., 2023)	LldR	Intensiometric (cmpApple) 559	1xCOX4	4 mM (*in situ*)	150 %	NA	NA
LACTATE/PYRUVATE								
Mito-lapronic	2020 (Galaz et al., 2020)	LutR	FRET (mTFP/Venus)	4x COX8	2 μM (Lac) 12.1 μM (Pyr)	15 %	140754	NA
PYRUVATE								
Mito-PyronicSF	2020 (Arce-Molina et al., 2020)	PdhR	Intensiometric (cpGFP) 488	1xCOX8	480 μM	60 %	124813	(Koshenov et al., 2022; Leung et al., 2024; Tiwari et al., 2024)
Mito-Pyronic	2020 (Arce-Molina et al., 2020)	PdhR	FRET (mTFP/Venus)	COX8	107 uM	40 %	NA	Rauseo et al. (2024)

[a] The maximum fluorescence response observed in mitochondria, as shown in the original paper. NA: not available.

Table 2
Krebs cycle fluorescent indicators tested in mammalian systems.

INDICATOR	YEAR	LIGAND BINDING MOIETY	READOUT	MITO TARGET	*IN VITRO* K_D	ΔF or ΔR_{MAX} (%) [a]	ADDGENE NUMBER	USERS
KREBS CYCLE METABOLITES								
ACETYL-CoA								
mito-PancACe	2024 (Smith et al., 2024)	PanZ	Intensiometric (SF, cpGFP)488	NA	274 μM	5 %	215710	NA
CITRATE								
mito-Citron1	2020 (Zhao et al., 2020)	CitA	Intensiometric(SF, GFP)488	2x COX8	1.1 mM	15 %	134305	(Koshenov et al., 2022; Madaris et al., 2023; Zhao et al., 2023)

[a] The maximum fluorescence response observed in mitochondria, as shown in the original paper. NA: not available.

5.3. Amino acid indicators

Structurally, amino acids are organic compounds containing both an amine (-NH2) and a carboxyl (-COOH) functional group, along with a unique side chain that defines their properties. Metabolically, they are the fundamental building blocks of proteins. Their importance in energy metabolism is twofold. First, when required as fuel, amino acids can be broken down, and their carbon skeletons are converted into key intermediates like pyruvate or acetyl-CoA, which then enter the Krebs cycle to be oxidized for ATP production. This process directly links protein catabolism to cellular respiration. Second, the Krebs cycle is a major anabolic hub, providing the necessary precursor molecules for the biosynthesis of many non-essential amino acids. This dual role makes amino acids central to both the catabolism and anabolism of molecules essential for cellular energy and cell structure.

As a specific example of monitoring an amino acid in mitochondria, the FHisJ a fluorescent indicator for histidine, was targeted to the matrix by fusing it with a 2xCOX8, creating FHisJ-Mit (Hu et al., 2017). This enabled the direct quantification of free histidine, revealing that in glucose-fed cells the mitochondrial concentration was significantly lower than the cytosol, while in glucose-deprived cells the levels were comparable. Furthermore, the targeted sensor was used to measure transport kinetics across the inner mitochondrial membrane with a K_m of approximately 55 μM. For a comprehensive view about the features of state-of-the-art GEFIs for amino acids that have been targeted to mitochondrial matrix and their users, see Table 3.

5.4. Cofactor indicators

Structurally, cofactors like NAD^+, NADH, $NADP^+$, and NADPH are dinucleotides, which are non-protein organic compounds essential for enzyme function. Metabolically, their importance is paramount. NAD^+ acts as a primary electron acceptor in catabolic pathways like glycolysis and the Krebs cycle, capturing high-energy electrons from the breakdown of nutrients to become its reduced form, NADH. This NADH is the crucial currency of energy metabolism, as it donates these electrons to the electron transport chain to power the synthesis of the vast majority of cellular ATP. In contrast, the NADPH/$NADP^+$ pair primarily provides reducing power for anabolic (biosynthetic) reactions. On the other hand, Coenzyme A is a classic example of a cofactor. Its primary role in energy metabolism is to act as a carrier for acyl groups, most notably forming acetyl-CoA. This molecule is the crucial link that feeds the two-carbon acetyl group, derived from the breakdown of carbohydrates and fats, into the Krebs cycle for oxidation.

While a variety of GEFIs for NADH and NAD^+ have been developed, their affinity for these cofactors is often too high for the concentrations known to exist in mitochondria. Specifically, mitochondrial matrix environment is more reduced by the constant production of NADH from the Krebs cycle reactions, therefore, within the mitochondrial its estimated concentrations are in the low millimolar range. Consequently,

Table 3
Amino acid fluorescent indicators tested in mammalian systems.

INDICATOR	YEAR	**LIGAND BINDING** MOIETY	READOUT	MITO TAG	*IN VITRO* K_D	ΔF or ΔR_{MAX} (%) [a]	Addgene	USERS
AMINOACIDS								
L-GLUTAMINE								
Mito-Gluta-R	2025 (Liu et al., 2025)	GlnBP	Ratiometric (cpYFP) 488/405	4x COX8	407.5 μM	50 %	NA	NA
L-HISTIDINE								
FHisJ-mit	2017 (Hu et al., 2017)	HisJ	Ratiometric (cp YFP) 485/420	2x COX8	22 μM	300 %	NA	Li et al. (2020)
L-LEUCINE-ISOLEUCINE AND VALINE								
mit-OLIVe	2019 (Yoshida et al., 2019)	LIVBP	FRET (YFP/CFP) 527/475	2x COX8	97 μM (Leu), 83 μM (isoleu) 589 μM (val)	90 %	NA	NA

[a] The maximum fluorescence response observed in mitochondria, as shown in the original paper. NA: not available.

fluorescent indicators with a high affinity with a dissociation constant (K_D) in the low micromolar range become fully saturated in this environment making it impractical for detection and monitoring. A saturated GEFI cannot accurately report the dynamic changes in cofactor concentration that are crucial for understanding metabolic state. This highlights a critical point in GEFIs design to work in mitochondria: it is not enough to simply target an indicator to the mitochondria efficiently; its detection range must also be carefully optimized to match the concentration of the analyte in that specific subcellular compartment. For a comprehensive view about the state-of-the-art of the current GEFIs for cofactors that have been targeted at mitochondrial matrix and their users, see Table 4.

5.5. *Energy nucleotide indicators*

Structurally, adenosine triphosphate (ATP) is a nucleoside triphosphate composed of adenine, a ribose sugar, and three phosphate groups linked by high-energy bonds. Metabolically, it serves as the universal "energy currency" of the cell, releasing energy for processes like muscle contraction and biosynthesis when hydrolyzed to adenosine diphosphate (ADP). Therefore, the ATP/ADP ratio is a critical sensor of the cell's energy status and a key metabolic regulator (Atkinson, 1968; Hardie et al., 2012). A high ATP/ADP ratio signals energy surplus, causing ATP to act as an allosteric inhibitor of key glycolytic enzymes like phosphofructokinase, thereby slowing energy production (Lynch et al., 2024; Passonneau and Lowry, 1964). Conversely, a low ratio (high ADP) signifies energy demand, causing ADP to act as an allosteric activator that stimulates glycolysis and oxidative phosphorylation to

Table 4
Cofactor fluorescent indicators tested in mammalian systems.

INDICATOR	YEAR OF PUBLICATION	LIGAND BINDING MOIETY	READOUT	MITO TARGET	*IN VITRO* K_D	ΔF or ΔR_{MAX} (%) [a]	ADDGENE NUMBER	USERS
COFACTOR INDICATORS								
NAD^+								
NAD + biosensor	2016 (Cambronne et al., 2016)	LigA	Ratiometric (cpVenus) 488/405	1x COX4	65 μM	40 %	186791	(Clark, A. J. et al., 2023; Clark et al., 2023; Eller et al., 2019; Gaudino et al., 2019; Goyal and Cambronne, 2022; Goyal et al., 2023; Hoyland et al., 2024; Lu et al., 2022; Luongo et al., 2020; Murata et al., 2019; Smith et al., 2019; Ward et al., 2019)
ChemoG-NAD	2023 (Hellweg et al., 2023)	LigA	FRET (eGFP/SiR)	COX8	200 μM	40 %	193823	NA
NADH/NAD^+								
mitoRexYFP	2014 (Bilan et al., 2014)	T-Rex	Ratiometric (cpYFP) 490	NA	180 nM (NADH)	30 %	60246	Chen et al. (2017)
mt-SoNar	2021 (Hu et al., 2021)	T-Rex	Ratiometric (cpYFP) 488/405	2x COX8	0.025 (K_R)	30 %	NA	(Balderas et al., 2022; Weiss-Sadan et al., 2023; Wu et al., 2022)
Mito-aY-SonaR	2020 (Zhang and Ai, 2020)	T-Rex	Intensiometric (aY induced cpYFP) 544	NA	0.025 (K_R)	40 %	NA	NA
NADH								
FREX-mit	2011(Zhao et al., 2011)	Rex	Ratiometric (cpYFP) 500/410	NA	3.7 μM	50 %	NA	(Li et al., 2023; Zhang et al., 2019; Zhao and Yang, 2016; Zhao et al., 2014; Zou et al., 2018)
NADPH								
iNap3-mit	2017 (Tao et al., 2017)	T-Rex	Ratiometric (cpYFP) 420/485	2 copies COX8	25.2 μM	50 %	NA	(Chen et al., 2022; Moon et al., 2020, 2024; Plecita-Hlavata et al., 2020)
Mito-aY-iNap1	2020 (Zhang and Ai, 2020)	T-Rex	Intensiometric (aY induced cpYFP) 545	NA	2 μM	40 %	NA	NA
NADP-NADPH								
NERST	2023 (Molinari et al., 2023)	NTRC	Ratiometric (roGFP2) 390/490	COX8	1 (K_R)	15 %	NA	NA
Coenzyme A								
CoaSnifit	2023 (Xue et al., 2023)	Pank	FRET (sfGFP/MaP) 510/580	NA	13.9 μM	40 %	197946	NA

[a] The maximum fluorescence response observed in mitochondria, as shown in the original paper. NA: not available.

regenerate ATP (Chance and Williams, 1955; Poorman et al., 1984). This feedback ensures cellular energy homeostasis.

ATP is the critical biochemical signal that connects the physical stimulus at the cell membrane to the cell's functional response. Utilizing single fluorophore GEFI mitAT1.03, to monitor ATP levels within the mitochondria of living cells, researchers observed that shear stress directly triggers a rapid surge in ATP synthesis inside the mitochondria. This newly generated ATP is then released from the cell, activating purinergic receptors on the cell surface, which initiates crucial Ca^{2+} signaling cascades. The investigation demonstrated that this entire mechanotransduction pathway, from the membrane cholesterol changes to the final calcium signa, is fundamentally dependent on the rapid increase in mitochondrial ATP, establishing its central role in the cell's response to blood flow. For a comprehensive view about the state-of-the-art of the current GEFIs for energy nucleotide that have been targeted at mitochondrial matrix and their users, see Table 5.

6. Consideration and challenges

The broad use of mitochondrially-targeted GEFIs is still in its infancy. Although the number of GEFIs for metabolites is increasing at a rapid pace, only a limited number of metabolites can be probed within the mitochondrial matrix using these fluorescence indicators. Major challenges arise from ensuring proper targeting to avoid leaky signals, and from uncertainties regarding how GEFI performance is affected by the structural modifications required for a correct mitochondrial targeting and the characteristic of the mitochondrial matrix environment. Specifically, it is often unclear how these factors influence the sensor's dynamic range, affinity, and detection limits. These parameters are critical not only for calibrating the fluorescent signal but also for achieving a semiquantitative interpretation of the data.

6.1. Calibrating GEFIs within the mitochondrial environment

While GEFIs provide excellent data on relative changes in metabolite levels, obtaining absolute quantitative concentrations requires accurate *in situ* calibration. This remains a significant challenge for mitochondrial-targeted sensors due to the unique and dynamic biochemical environment of the matrix, which is difficult to replicate *in vitro*. Current methods often involve permeabilizing the plasma membrane with detergents like digitonin, followed by exposing the fluorescent indicator to known concentrations of the metabolite. However, permeabilization can alter the cytosolic environment and by extension ion gradients, cofactor levels, pH into the mitochondria. Therefore, these conditions may not fully reflect the conditions experienced by the GEFI in an intact mitochondrion. The main challenge is the validation of the K_D and the dynamic range of mitochondrial targeted GEFIs, to design one or two-point calibration strategies. Unfortunately, these parameters are obtained from the *in vitro* experiments using purified protein, experimental conditions that do not fully reflect the mitochondrial environment. More specifically, one-point calibration strategies needs K_D and dynamic range of fluorescent indicators, which implies the use of two parameters with high degree of uncertainties. On the other hand, two-point calibration strategies use only the *in vitro* K_D implying that both apo and saturated state of the GEFI was achieved. Due to metabolic constraints and our poor current knowledge about mitochondrial metabolite transport and permeability, saturation point of a given GEFIs is difficult to achieve and validate. Therefore, the dynamic range that is used to calculate the metabolites concentration carry a high degree of uncertainty. Calibrated data from GEFIs targeted to mitochondria must be interpreted with caution. Developing less invasive and more reliable *in situ* calibration techniques with fluorescent indicators with differential affinity for the analyte to perform cross calibration protocols, is a key area for advancement to unlock the full quantitative potential of mitochondrial GEFIs and improve the parameterization of metabolic models.

6.2. pH sensitivity and fluorescent protein artifacts

The distinct environment of the mitochondrial matrix can also directly influence the fluorescent properties of the FP component of a GEFI, independent of metabolite binding. For example, the matrix pH is typically more alkaline than the cytosol ranging from 7.6 to as high as 8.0 under energized conditions. Many FPs are pH-sensitive (Aburto et al., 2022; Arce-Molina et al., 2020; Tantama et al., 2013; Tao et al., 2017; Zhao et al., 2011), if not accounted for, such pH-induced fluorescence changes could be misinterpreted as changes in metabolite concentration. This underscores the need for careful fluorescent indicator characterization within the mitochondrial context and the selection of FPs known for their robustness or the use of ratiometric approaches that can mitigate such artifacts.

The fluorescence mechanism in many fluorescent proteins (FPs) is initiated by an excitation event that triggers an excited-state proton transfer. This process involves the transition of the chromophore between its protonated and deprotonated states and is necessary to complete the excitation-emission cycle. The pKa of fluorescent proteins, which defines the pH at which the chromophore is 50 % protonated, varies widely from approximately 4.5 to over 12, depending on the specific variant. This value is a crucial characteristic, as the transition between protonated and deprotonated states directly impacts fluorescence. Consequently, GEFIs based on FPs with a pKa far from physiological pH (cytosolic ~7.4 and mitochondrial ~7.8) will be insensitive to proton fluctuations in this range. This is the case for GEFIs based on cyan fluorescent proteins such as Cerulean with a pKa = 4.7 (Rizzo et al., 2004) or mTurquoise2 with a pKa = 3.1 (Goedhart et al., 2012). Among green fluorescent proteins, an acid-resistant variant named Gamillus was recently isolated from the flower hat jelly, *Olindias formosa* (Shinoda et al., 2018). This FP presents exceptional acid resistance, with a pKa of 3.4, making Gamillus a prime candidate for engineering novel acid-resistant, single-fluorophore biosensors. However, the proton sensitivity of a GEFI does not rely solely on the FP. It can also arise from the ligand-sensing domain or be an emergent property of the final chimeric protein. Eliminating this confounding factor is challenging. One successful strategy involves using random mutagenesis to identify variants with reduced proton sensitivity in the physiological range (Hung et al., 2011; Koveal et al., 2022). Nevertheless, pH-induced artifacts can be distinguished from the true sensor response by using several control strategies. These include employing non-responsive or "dead" variants of the GEFI (Arce-Molina et al., 2020), performing ratiometric measurements at two different excitation wavelengths (Tao et al., 2017), utilizing the proton-insensitive isosbestic point of the fluorophore and coexpressing and targeting to mitochondria a proton-sensitive fluorescent protein (Liu et al., 2021; Poburko et al., 2011).

6.3. Potential buffering effects of high-affinity GEFIs

The GEFI itself, if it binds its target metabolite with very high affinity and is present at high concentrations, could act as a buffer or sink for the metabolite, thereby perturbing its natural dynamics and altering its free concentration or kinetics. This phenomenon has been a long-recognized concern, particularly for the widely used GCaMP and iGluSnFR family of calcium and glutamate fluorescent indicators, respectively. High concentrations of GCaMP can blunt natural calcium spikes and iGluSnFR can significantly reduce the concentration of glutamate that reaches postsynaptic receptors, directly altering synaptic transmission and plasticity (Helassa et al., 2018). These leads to an underestimation of physiological signaling events and potentially altering downstream cellular processes. It is generally advisable to use the lowest possible expression levels that still provide adequate signal-to-noise, and to include appropriate controls, such as expressing a non-responsive or catalytically inactive version of the sensor, to assess potential non-specific effects on mitochondrial or cellular physiology. The

Table 5
Energy nucleotides fluorescent indicators tested in mammalian systems.

INDICATOR	YEAR	LIGAND BINDING MOIETY	READOUT	MITO TARGET	*IN VITRO* K_D	ΔF or ΔR_{MAX} (%) [a]	ADGENE NUMBER	USER
ENERGY NUCLEOTIDES								
ATP								
mit-GO-Ateam2	2011 (Nakano et al., 2011)	Ɛ subunit FoF1-ATP synthase	FRET (GFP/OFP) 560/510	NA	2.3 mM	40 %	NA	(Agarwal and Ganesh, 2020; Chamberlain et al., 2021; Choi et al., 2023; Dominguez-Zorita et al., 2023; Golombek et al., 2024; Golombek et al., 2023; Lefkimmiatis et al., 2013; N'Gadjaga et al., 2022; Richetin et al., 2020; Rueda et al., 2015; Shibata et al., 2015; Spurlock et al., 2019; Spurlock and Mitra, 2021; Tanaka et al., 2014; Writzl et al., 2017; Zhao et al., 2022; Zhou et al., 2016)
mit-ATeam1.03	2009 (Imamura et al., 2009)	Ɛ subunit FoF1-ATP synthase	FRET (mseCFP/cp173Venus) 527/475	2x COX8	3.3 mM	100 %	NA	(Barsukova et al., 2011; Bischof et al., 2021; Bischof et al., 2024; Charles et al., 2017; Chen et al., 2019; Choi et al., 2022; De Marchi et al., 2011; Depaoli et al., 2018; Forkink et al., 2014; Fouque et al., 2016; Fouquerel et al., 2014; Goehring et al., 2012; Gouriou et al., 2020; Gross et al., 2022; Han et al., 2021; Hayashi et al., 2015; J et al., 2013; Jia et al., 2024; Kamikubo et al., 2019; Kealey et al., 2022; Kennedy et al., 2014; Kioka et al., 2014; Kioka et al., 2020; Koshenov et al., 2021; Lee et al., 2022; Lee et al., 2019; Lucantoni et al., 2018a; Lucantoni et al., 2018b; Lucantoni et al., 2021; Ludtmann et al., 2016; Ludtmann et al., 2017; Madreiter-Sokolowski et al., 2016; Matsuda et al., 2020; Nagai et al., 2017; Nagao et al., 2020; Nakamura et al., 2023; Nakano et al., 2017; Neary et al., 2014; Nerlich et al., 2018; Oflaz et al., 2022; Pavlyuchenkova et al., 2022; Pilic et al., 2024; Quintana-Cabrera et al., 2021; Quintana-Cabrera et al., 2018; Rauter et al., 2020a; Rauter et al., 2020b; Rossi et al., 2020; Satoh et al., 2023; Shindo et al., 2016; Shintani et al., 2014; Suzuki et al., 2018; Trinh et al., 2019; van der Stel et al., 2022; van Hameren et al., 2018; van Hameren et al., 2019; Vishnu et al., 2014; Waldeck-Weiermair et al., 2011; Watanabe et al., 2022; Wilde et al., 2020; Wilde et al., 2019; Wright et al., 2016; Xie et al., 2017; Xie et al., 2016; Xue et al., 2023; Yamamoto et al., 2018; Yamamoto et al., 2020; Yamamoto et al., 2023; Yong et al., 2019; Zaninello et al., 2024; Zhao et al., 2019)
mito-eATeam	2023 (Sahan et al., 2023)	Ɛ subunit FoF1-ATP synthase	FRET (Ypet/mCerulean)	dAKAP	3.3 mM	20 %	NA	NA
mito-iATPSnFR2	2024 (Marvin et al., 2024)	Ɛ subunit FoF1-ATP synthase	cpSFEGFP	4x COX8	0.5 mM	50 %	214925	NA
mitoMaLionR	2018 (Arai et al., 2018)	Ɛ subunit FoF1-ATP synthase	mApple 565	1x COX8	2 mM	10 %	NA	(Ferdinandus et al., 2022; Lauterboeck et al., 2024; Tsuno et al., 2024; White et al., 2023; Zhao et al., 2020)
mitoMaLionG	2018 (Arai et al., 2018)	Ɛ subunit FoF1-ATP synthase	GFP citrine variant 505	1x COX8	2 mM	NA	NA	NA
qMaLioffG (flim)	2023 (Arai et al., 2023)	Ɛ subunit FoF1-ATP synthase	citrine	NA	2.2 mM	10 %	NA	NA
smacATPi	2023 (White et al., 2023)	Ɛ subuni FoF1-ATP synthase	GFP Citrine variant (cyto) and mApple (mito)	1x COX8	2 mM	10–30 %	NA	NA
GTP/GDP								
GRISerHR	2022 (Zhang et al., 2022)	eIF5B	Ratiometric (cpYFP) 488/405	4x COX8	3 μM	20 %	NA	NA
ATP/ADP								
RNb-PercevalHR	2013 (Tantama et al., 2013)	GlnK	Ratiometric (RFP) 405/488	NA	3.5 (K_R)	100 %	NA	NA

[a] The maximum fluorescence response observed in mitochondria, as shown in the original paper. NA: not available.

expression of any exogenous protein within mitochondria can potentially alter organellar physiology. They may also impose a metabolic load on the cell due to the energy costs of synthesis, import, and folding, or could interfere with the mitochondrial protein import machinery or other protein interactions. This "observer effect" is a subtle but critical concern, particularly when multiple GEFIs are co-expressed or when very large and complex sensor constructs are used. Also, the process of chromophore maturation induces the generation of H_2O_2, which could produce changes in the protein and metabolic profile (Barakat et al., 2024). Strategies to mitigate this include using strong MTS sequences coupled with weaker, regulatable promoters to achieve the lowest effective sensor concentration, developing brighter sensors that require lower expression levels for adequate signal and use dead fluorescent indicators to confirm that an observed effect is due to the target molecule and not some other artifact of protein overexpression. A "metabolite-dead" or non-responsive version of the fluorescent indicators can be expressed as a control. If a cellular process is altered in the presence of fluorescent indicators but not the dead version, it provides strong evidence that the effect is due to metabolite buffering itself.

6.4. Mitochondrial import efficiency and localization

The mitochondrial import machinery is optimized for native mitochondrial proteins, which have co-evolved with the import apparatus. GEFIs, which are often large fusion proteins, can be difficult substrates for this machinery to handle. However, the frequent use of tandem repeats suggests that importing large, engineered proteins like GEFIs demands the use of tandem MTS repeats. Therefore, a single MTS copy may not always suffice for efficient targeting, especially for FRET-based fluorescent indicators. Additionally, high protein expression levels within mitochondria is not without potential consequences. It could produce saturation of the mitochondrial import systems inducing an increase leakage to the cytosol. Also, the expression of a foreign protein, particularly a relatively large one like a GEFI, can impose a burden on the mitochondrial protein import machinery, consume ATP and membrane potential during import, and potentially interfere with normal mitochondrial processes or proteostasis. In this regard, modern fluorescent proteins used to engineer GEFIs still display brightness levels that demand mild to high expression levels to reach workable signal-to-noise ratio. Therefore, leakage towards the cytosol should be always expected and controlled. On the other hand, the size and tertiary structure of the GEFI can influence its import efficiency. Large, bulky, or rapidly folding proteins may be translocated less efficiently across the mitochondrial membranes. As mentioned before, using multiple MTS copies or optimizing linker regions between the MTS and the GEFI are common strategies to improve mitochondrial import (Galanis et al., 1991; Thornton et al., 1993). Despite the presence of multiple MTS, a fraction of the GEFI might still remain in the cytosol or be mis-localized to other cellular compartments. This can occur due to inefficient import, saturation of the import machinery, the presence of cryptic alternative translation start sites, or "leaky" targeting. Rigorous validation of correct mitochondrial localization, typically through colocalization studies with established mitochondrial markers e.g., MitoTracker dyes, or immunofluorescence against endogenous mitochondrial proteins like TOM20 or HSP60, is essential to ensure that the recorded signals indeed originate from mitochondria.

7. Perspectives

7.1. Multiplexed imaging of metabolites in mitochondria

The development of GEFIs with diverse spectral characteristics e.g., green, yellow, red, and far-red variants, is crucial to face these challenges. This allows researchers to co-express and image multiple GEFIs reporting on different metabolites, or to combine a metabolite GEFIs with fluorescent indicators for other critical parameters like mitochondrial Ca^{2+}, pH, membrane potential, or reactive oxygen species. Such multiplexed imaging provides a more holistic view of mitochondrial regulation and its coordination with broader cellular events. We envision that development and optimization of GEFIs paralleled by advancements in fluorescence microscopy techniques, including Fluorescence Life-Time Imaging (FLIM), super-resolution microscopy, and multiphoton microscopy will make synergy that help to continually expand the horizons of live-cell imaging, facilitating increasingly complex experimental designs, such as the simultaneous monitoring of multiple metabolic parameters with sub-cellular resolution. Understanding these requires the simultaneous measurement of multiple parameters.

7.2. In-vivo models

Extending the use of mitochondrially-targeted GEFIs from cell culture models to living tissues and whole organisms is a major frontier. This transition presents challenges related to efficient and cell-type-specific sensor delivery (e.g., using viral vectors or generating transgenic animals), imaging depth in scattering tissues, maintaining physiological conditions during imaging, and achieving adequate signal-to-noise ratios. However, *in vivo* applications are essential for understanding how mitochondrial metabolism is regulated in the context of complex tissue architecture, intercellular communication, and whole-body physiology in both health and disease. A recent study assessing the mitochondrial lactate pool *in vivo* using mito-CanlonicSF demostrates that mitochondrial lactate in neurons covaries with plasma lactate, a finding that opens up new questions about how exercise impacts neuronal physiology (Rauseo et al., 2024).

7.3. Synergy with advanced imaging technologies

The future of mitochondrial research lies in observing metabolism not as a static snapshot, but as a dynamic process unfolding within the complex architecture of living tissues. The convergence of genetically encoded indicators with a new generation of imaging technologies is paving the way for this paradigm shift. Looking forward, Light-Sheet Microscopy stands to revolutionize our understanding of metabolic programming during development; its inherent gentleness and speed are now enabling the tracking of ATP dynamics across entire organoids and embryos, offering unprecedented views of cellular decision-making (Chhhetri et al., 2022). This capability is complemented by Multiphoton Microscopy, which pushes the frontier of observation into living animals, allowing us to finally witness how mitochondrial redox states respond to real-world physiological events in deep tissues like the brain (Tantama et al., 2013). Perhaps most critically, Fluorescence Lifetime Imaging (FLIM) is solving the persistent challenge of robust quantification. By providing readouts independent of sensor expression levels, FLIM is transforming FRET-based biosensors into highly precise tools, capable of mapping subtle, yet crucial, metabolic vulnerabilities within complex disease models like cancer spheroids (Knowles et al., 2021). The integration of these synergistic approaches is no longer a distant goal but a current reality, promising to unlock a truly holistic understanding of mitochondrial function in health and disease.

8. Conclusion

Mitochondria are more than the cell's powerhouse. They participate in numerous physiological and pathophysiological processes. To decipher the regulatory mechanisms underlying mitochondrial function, the organelle must be examined *in situ*, where its native metabolic and structural interactions remain intact. GEFIs for metabolites are promising tools, though still in an early stage of development. Expanding the repertoire of mitochondrial metabolites that can be probed and optimizing existing indicators will provide a more comprehensive view of metabolism at subcellular resolution in living systems.

CRediT authorship contribution statement

C. Aburto: Writing – review & editing, Writing – original draft, Data curation. **A. Pinilla:** Data curation. **F. Carrera-Arenas:** Data curation. **A. San Martín:** Writing – review & editing, Writing – original draft, Validation, Supervision, Data curation, Conceptualization.

AI use statement

During the preparation of this work the author(s) used Gemini in order to enhance the language and clarity of the text. After using this tool/service, the author(s) reviewed and edited the content as needed and take(s) full responsibility for the content of the publication.

Funding

The authors declare that no funds, grants, or other support were received during the preparation of this manuscript.

Declaration of competing interest

The authors declare that there are no financial, personal, or professional conflicts of interest that could be perceived as having influenced the research presented in this manuscript. All funding sources and any potential conflicts have been fully disclosed in the Funding section. Each author has contributed significantly to the work, has reviewed and approved the final version of the manuscript, and agrees with its submission.

Acknowledgment

We thank the members of the Energy Metabolism Group at CECs. Schematic representations were created in BioRender, https://BioRender.com/hhfdqjd.

Data availability

No data was used for the research described in the article.

References

Aburto, C., Galaz, A., Bernier, A., Sandoval, P.Y., Holtheuer-Gallardo, S., Ruminot, I., Soto-Ojeda, I., Hertenstein, H., Schweizer, J.A., Schirmeier, S., Pastor, T.P., Mardones, G.A., Barros, L.F., San Martin, A., 2022. Single-fluorophore indicator to explore cellular and sub-cellular lactate dynamics. ACS Sens. 7 (11), 3278–3286.

Agarwal, S., Ganesh, S., 2020. Perinuclear mitochondrial clustering, increased ROS levels, and HIF1 are required for the activation of HSF1 by heat stress. J Cell Sci 133 (13).

Akerboom, J., Rivera, J.D., Guilbe, M.M., Malave, E.C., Hernandez, H.H., Tian, L., Hires, S.A., Marvin, J.S., Looger, L.L., Schreiter, E.R., 2009. Crystal structures of the GCaMP calcium sensor reveal the mechanism of fluorescence signal change and aid rational design. J. Biol. Chem. 284 (10), 6455–6464.

Arai, S., Itoh, H., Vu, C.Q., Nakayama, M., Oshima, M., Morita, A., Okamoto, K., Okuda, S., Teranishi, A., Osawa, M., Tamura, Y., Nonoyama, S., Takuma, M., Fujie, T., Sarker, S.R., Sudhaharan, T., Kiya, T., Lane, E.B., Kitaguchi, T., 2023. qMaLioffG: a single green fluorescent protein FLIM indicator enabling quantitative imaging of endogenous ATP. bioRxiv, 2023.2008.2029.555275.

Arai, S., Kriszt, R., Harada, K., Looi, L.S., Matsuda, S., Wongso, D., Suo, S., Ishiura, S., Tseng, Y.H., Raghunath, M., Ito, T., Tsuboi, T., Kitaguchi, T., 2018. RGB-color intensiometric indicators to visualize spatiotemporal dynamics of ATP in single cells. Angew Chem. Int. Ed. Engl. 57 (34), 10873–10878.

Arce-Molina, R., Cortes-Molina, F., Sandoval, P.Y., Galaz, A., Alegria, K., Schirmeier, S., Barros, L.F., San Martin, A., 2020. A highly responsive pyruvate sensor reveals pathway-regulatory role of the mitochondrial pyruvate carrier MPC. eLife 9.

Ast, C., Foret, J., Oltrogge, L.M., De Michele, R., Kleist, T.J., Ho, C.H., Frommer, W.B., 2017. Ratiometric Matryoshka biosensors from a nested cassette of green- and orange-emitting fluorescent proteins. Nat. Commun. 8 (1), 431.

Atkinson, D.E., 1968. The energy charge of the adenylate pool as a regulatory parameter. Interaction with feedback modifiers. Biochemistry 7 (11), 4030–4034.

Baird, G.S., Zacharias, D.A., Tsien, R.Y., 1999. Circular permutation and receptor insertion within green fluorescent proteins. Proc. Natl. Acad. Sci. U. S. A. 96 (20), 11241–11246.

Balderas, E., Eberhardt, D.R., Lee, S., Pleinis, J.M., Sommakia, S., Balynas, A.M., Yin, X., Parker, M.C., Maguire, C.T., Cho, S., Szulik, M.W., Bakhtina, A., Bia, R.D., Friederich, M.W., Locke, T.M., Van Hove, J.L.K., Drakos, S.G., Sancak, Y., Tristani-Firouzi, M., Franklin, S., Rodan, A.R., Chaudhuri, D., 2022. Mitochondrial calcium uniporter stabilization preserves energetic homeostasis during complex I impairment. Nat. Commun. 13 (1), 2769.

Barakat, S., Cimen, S., Miri, S.M., Vatandaslar, E., Yelkenci, H.E., San Martin, A., Beker, M.C., Kok, K., Ozturk, G., Eroglu, E., 2024. Bioenergetic shift and proteomic signature induced by lentiviral-transduction of GFP-based biosensors. Redox Biol. 78, 103416.

Barsukova, A.G., Bourdette, D., Forte, M., 2011. Mitochondrial calcium and its regulation in neurodegeneration induced by oxidative stress. Eur. J. Neurosci. 34 (3), 437–447.

Bilan, D.S., Matlashov, M.E., Gorokhovatsky, A.Y., Schultz, C., Enikolopov, G., Belousov, V.V., 2014. Genetically encoded fluorescent indicator for imaging NAD(+)/NADH ratio changes in different cellular compartments. Biochim. Biophys. Acta 1840 (3), 951–957.

Birsoy, K., Wang, T., Chen, W.W., Freinkman, E., Abu-Remaileh, M., Sabatini, D.M., 2015. An essential role of the mitochondrial electron transport chain in cell proliferation is to enable aspartate synthesis. Cell 162 (3), 540–551.

Bischof, H., Burgstaller, S., Graier, W.F., Lukowski, R., Malli, R., 2021. Unveiling the K(+)-sensitivity of cell metabolism using genetically encoded, FRET-based K(+), glucose, and ATP biosensors. STAR Protoc 2 (4), 100843.

Bischof, H., Maier, S., Koprowski, P., Kulawiak, B., Burgstaller, S., Jasinska, J., Serafimov, K., Zochowska, M., Gross, D., Schroth, W., Matt, L., Juarez Lopez, D.A., Zhang, Y., Bonzheim, I., Buttner, F.A., Fend, F., Schwab, M., Birkenfeld, A.L., Malli, R., Lammerhofer, M., Bednarczyk, P., Szewczyk, A., Lukowski, R., 2024. mitoBK(Ca) is functionally expressed in murine and human breast cancer cells and potentially contributes to metabolic reprogramming. eLife 12.

Boveris, A., Chance, B., 1973. The mitochondrial generation of hydrogen peroxide. General properties and effect of hyperbaric oxygen. Biochem. J. 134 (3), 707–716.

Braunstein, A.E., Kritzmann, M.G., 1937. Formation and breakdown of amino-acids by inter-molecular transfer of the amino Group. Nature 140 (3542), 503–504.

Bricker, D.K., Taylor, E.B., Schell, J.C., Orsak, T., Boutron, A., Chen, Y.C., Cox, J.E., Cardon, C.M., Van Vranken, J.G., Dephoure, N., Redin, C., Boudina, S., Gygi, S.P., Brivet, M., Thummel, C.S., Rutter, J., 2012. A mitochondrial pyruvate carrier required for pyruvate uptake in yeast, Drosophila, and humans. Science 337 (6090), 96–100.

Brooks, G.A., 1986. The lactate shuttle during exercise and recovery. Med. Sci. Sports Exerc. 18 (3), 360–368.

Brooks, G.A., 2018. The science and translation of lactate shuttle theory. Cell Metab. 27 (4), 757–785.

Cambronne, X.A., Stewart, M.L., Kim, D., Jones-Brunette, A.M., Morgan, R.K., Farrens, D. L., Cohen, M.S., Goodman, R.H., 2016. Biosensor reveals multiple sources for mitochondrial NAD(+). Science 352 (6292), 1474–1477.

Chamberlain, K.A., Huang, N., Xie, Y., LiCausi, F., Li, S., Li, Y., Sheng, Z.H., 2021. Oligodendrocytes enhance axonal energy metabolism by deacetylation of mitochondrial proteins through transcellular delivery of SIRT2. Neuron 109 (21), 3456–3472 e3458.

Chance, B., Williams, G.R., 1955. Respiratory enzymes in oxidative phosphorylation. III. The steady state. J. Biol. Chem. 217 (1), 409–427.

Charles, E., Hammadi, M., Kischel, P., Delcroix, V., Demaurex, N., Castelbou, C., Vacher, A.M., Devin, A., Ducret, T., Nunes, P., Vacher, P., 2017. The antidepressant fluoxetine induces necrosis by energy depletion and mitochondrial calcium overload. Oncotarget 8 (2), 3181–3196.

Chen, C., Lai, X., Zhang, Y., Xie, L., Yu, Z., Dan, S., Jiang, Y., Chen, W., Liu, L., Yang, Y., Huang, D., Zhao, Y., Zheng, J., 2022. NADPH metabolism determines the leukemogenic capacity and drug resistance of AML cells. Cell Rep. 39 (1), 110607.

Chen, H., Xu, H., Potash, S., Starkov, A., Belousov, V.V., Bilan, D.S., Denton, T.T., Gibson, G.E., 2017. Mild metabolic perturbations alter succinylation of mitochondrial proteins. J. Neurosci. Res. 95 (11), 2244–2252.

Chen, W., Xue, Y., Scarfe, L., Wang, D., Zhang, Y., 2019. Loss of prune in circadian cells decreases the amplitude of the circadian locomotor rhythm in drosophila. Front. Cell. Neurosci. 13, 76.

Chen, W.W., Freinkman, E., Wang, T., Birsoy, K., Sabatini, D.M., 2016. Absolute quantification of matrix metabolites reveals the dynamics of mitochondrial metabolism. Cell 166 (5), 1324–1337 e1311.

Choi, J., Matoba, N., Setoyama, D., Watanabe, D., Ohnishi, Y., Yasui, R., Kitai, Y., Oomachi, A., Kotobuki, Y., Nishiya, Y., Pieper, M.P., Imamura, H., Yanagita, M., Yamamoto, M., 2023. The SGLT2 inhibitor empagliflozin improves cardiac energy status via mitochondrial ATP production in diabetic mice. Commun. Biol. 6 (1), 278.

Choi, M.L., Chappard, A., Singh, B.P., Maclachlan, C., Rodrigues, M., Fedotova, E.I., Berezhnov, A.V., De, S., Peddie, C.J., Athauda, D., Virdi, G.S., Zhang, W., Evans, J.R., Wernick, A.I., Zanjani, Z.S., Angelova, P.R., Esteras, N., Vinokurov, A.Y., Morris, K., Jeacock, K., Tosatto, L., Little, D., Gissen, P., Clarke, D.J., Kunath, T., Collinson, L., Klenerman, D., Abramov, A.Y., Horrocks, M.H., Gandhi, S., 2022. Pathological structural conversion of alpha-synuclein at the mitochondria induces neuronal toxicity. Nat. Neurosci. 25 (9), 1134–1148.

Clark, A.J., Saade, M.C., Vemireddy, V., Vu, K.Q., Flores, B.M., Etzrodt, V., Ciampa, E.J., Huang, H., Takakura, A., Zandi-Nejad, K., Zsengeller, Z.K., Parikh, S.M., 2023a. Hepatocyte nuclear factor 4alpha mediated quinolinate phosphoribosylltransferase (QPRT) expression in the kidney facilitates resilience against acute kidney injury. Kidney Int. 104 (6), 1150–1163.

Clark, A.J., Saade, M.C., Vemireddy, V., Vu, K.Q., Flores, B.M., Etzrodt, V., Ciampa, E.J., Huang, H., Takakura, A., Zandi-Nejad, K., Zsengellér, Z.K., Parikh, S.M., 2023b. HNF4α mediated QPRT expression in the kidney facilitates resilience against acute kidney injury. bioRxiv, 2023.2005.2023.541987.

Day, R.N., Booker, C.F., Periasamy, A., 2008. Characterization of an improved donor fluorescent protein for forster resonance energy transfer microscopy. J. Biomed. Opt. 13 (3), 031203.
De Marchi, U., Castelbou, C., Demaurex, N., 2011. Uncoupling protein 3 (UCP3) modulates the activity of sarco/endoplasmic reticulum Ca2+-ATPase (SERCA) by decreasing mitochondrial ATP production. J. Biol. Chem. 286 (37), 32533–32541.
Depaoli, M.R., Karsten, F., Madreiter-Sokolowski, C.T., Klec, C., Gottschalk, B., Bischof, H., Eroglu, E., Waldeck-Weiermair, M., Simmen, T., Graier, W.F., Malli, R., 2018. Real-time imaging of mitochondrial ATP dynamics reveals the metabolic setting of single cells. Cell Rep. 25 (2), 501–512 e503.
Dominguez-Zorita, S., Romero-Carraminana, I., Santacatterina, F., Esparza-Molto, P.B., Simo, C., Del-Arco, A., Nunez de Arenas, C., Saiz, J., Barbas, C., Cuezva, J.M., 2023. IF1 ablation prevents ATP synthase oligomerization, enhances mitochondrial ATP turnover and promotes an adenosine-mediated pro-inflammatory phenotype. Cell Death Dis. 14 (7), 413.
Eilers, M., Hwang, S., Schatz, G., 1988. Unfolding and refolding of a purified precursor protein during import into isolated mitochondria. EMBO J. 7 (4), 1139–1145.
Eller, J.M., Stewart, M.L., Slepian, A.J., Markwardt, S., Wiedrick, J., Cohen, M.S., Goodman, R.H., Cambronne, X.A., 2019. Flow cytometry analysis of free intracellular NAD(+) using a targeted biosensor. Curr. Protoc. Cytom. 88 (1), e54.
Fehr, M., Frommer, W.B., Lalonde, S., 2002. Visualization of maltose uptake in living yeast cells by fluorescent nanosensors. Proc. Natl. Acad. Sci. U. S. A. 99 (15), 9846–9851.
Ferdinandus, Suzuki, M., Vu, C.Q., Harada, Y., Sarker, S.R., Ishiwata, S., Kitaguchi, T., Arai, S., 2022. Modulation of local cellular activities using a photothermal dye-based subcellular-sized heat spot. ACS Nano 16 (6), 9004–9018.
Forkink, M., Manjeri, G.R., Liemburg-Apers, D.C., Nibbeling, E., Blanchard, M., Wojtala, A., Smeitink, J.A., Wieckowski, M.R., Willems, P.H., Koopman, W.J., 2014. Mitochondrial hyperpolarization during chronic complex I inhibition is sustained by low activity of complex II, III, IV and V. Biochim. Biophys. Acta 1837 (8), 1247–1256.
Fouque, A., Lepvrier, E., Debure, L., Gouriou, Y., Malleter, M., Delcroix, V., Ovize, M., Ducret, T., Li, C., Hammadi, M., Vacher, P., Legembre, P., 2016. The apoptotic members CD95, BclxL, and Bcl-2 cooperate to promote cell migration by inducing Ca (2+) flux from the endoplasmic reticulum to mitochondria. Cell Death Differ. 23 (10), 1702–1716.
Fouquerel, E., Goellner, E.M., Yu, Z., Gagne, J.P., Barbi de Moura, M., Feinstein, T., Wheeler, D., Redpath, P., Li, J., Romero, G., Migaud, M., Van Houten, B., Poirier, G. G., Sobol, R.W., 2014. ARTD1/PARP1 negatively regulates glycolysis by inhibiting hexokinase 1 independent of NAD+ depletion. Cell Rep. 8 (6), 1819–1831.
Frei, M.S., Mehta, S., Zhang, J., 2024. Next-generation genetically encoded fluorescent biosensors illuminate cell signaling and metabolism. Annu. Rev. Biophys. 53 (1), 275–297.
Galanis, M., Devenish, R.J., Nagley, P., 1991. Duplication of leader sequence for protein targeting to mitochondria leads to increased import efficiency. FEBS Lett. 282 (2), 425–430.
Galaz, A., Cortes-Molina, F., Arce-Molina, R., Romero-Gomez, I., Mardones, G.A., Felipe Barros, L., San Martin, A., 2020. Imaging of the lactate/pyruvate ratio using a genetically encoded forster resonance energy transfer indicator. Anal. Chem. 92 (15), 10643–10650.
Gaudino, F., Manfredonia, I., Manago, A., Audrito, V., Raffaelli, N., Vaisitti, T., Deaglio, S., 2019. Subcellular characterization of nicotinamide adenine dinucleotide biosynthesis in metastatic melanoma by using organelle-specific biosensors. Antioxidants Redox Signal. 31 (15), 1150–1165.
Gavel, Y., Nilsson, L., von Heijne, G., 1988. Mitochondrial targeting sequences. Why 'non-amphiphilic' peptides May still be amphiphilic. FEBS Lett. 235 (1–2), 173–177.
Goedhart, J., von Stetten, D., Noirclerc-Savoye, M., Lelimousin, M., Joosen, L., Hink, M. A., van Weeren, L., Gadella Jr., T.W., Royant, A., 2012. Structure-guided evolution of cyan fluorescent proteins towards a quantum yield of 93%. Nat. Commun. 3, 751.
Goehring, I., Gerencser, A.A., Schmidt, S., Brand, M.D., Mulder, H., Nicholls, D.G., 2012. Plasma membrane potential oscillations in insulin secreting Ins-1 832/13 cells do not require glycolysis and are not initiated by fluctuations in mitochondrial bioenergetics. J. Biol. Chem. 287 (19), 15706–15717.
Golombek, M., Tsigaras, T., Schaumkessel, Y., Hansch, S., Weidtkamp-Peters, S., Anand, R., Reichert, A.S., Kondadi, A.K., 2024. Cristae dynamics is modulated in bioenergetically compromised mitochondria. Life Sci. Alliance 7 (2).
Golombek, M., Tsigaras, T., Schaumkessel, Y., Hänsch, S., Weidtkamp-Peters, S., Anand, R., Reichert, A.S., Kondadi, A.K., 2023. Live-cell super-resolution nanoscopy reveals modulation of cristae dynamics in bioenergetically compromised mitochondria. bioRxiv, 2023.2004.2027.538553.
Gouriou, Y., Alam, M.R., Harhous, Z., Crola Da Silva, C., Baetz, D.B., Badawi, S., Lefai, E., Rieusset, J., Durand, A., Harisseh, R., Gharib, A., Ovize, M., Bidaux, G., 2020. ANT2-Mediated ATP import into mitochondria protects against hypoxia lethal injury. Cells 9 (12).
Goyal, S., Cambronne, X.A., 2022. Dynamics of mitochondrial NAD^+ import reveal preference for oxidized ligand and substrate led transport. bioRxiv, 2022.2011.2004.515224.
Goyal, S., Paspureddi, A., Lu, M.J., Chan, H.R., Lyons, S.N., Wilson, C.N., Niere, M., Ziegler, M., Cambronne, X.A., 2023. Dynamics of SLC25A51 reveal preference for oxidized NAD(+) and substrate led transport. EMBO Rep. 24 (10), e56596.
Gross, D., Bischof, H., Maier, S., Sporbeck, K., Birkenfeld, A.L., Malli, R., Ruth, P., Proikas-Cezanne, T., Lukowski, R., 2022. IK(Ca) channels control breast cancer metabolism including AMPK-driven autophagy. Cell Death Dis. 13 (10), 902.
Han, S., Zhang, M., Jeong, Y.Y., Margolis, D.J., Cai, Q., 2021. The role of mitophagy in the regulation of mitochondrial energetic status in neurons. Autophagy 17 (12), 4182–4201.
Hardie, D.G., Ross, F.A., Hawley, S.A., 2012. AMPK: a nutrient and energy sensor that maintains energy homeostasis. Nat. Rev. Mol. Cell Biol. 13 (4), 251–262.
Haskins, N., Bhuvanendran, S., Anselmi, C., Gams, A., Kanholm, T., Kocher, K.M., LoTempio, J., Krohmaly, K.I., Sohai, D., Stearrett, N., Bonner, E., Tuchman, M., Morizono, H., Jaiswal, J.K., Caldovic, L., 2020. Mitochondrial enzymes of the urea cycle cluster at the inner mitochondrial membrane. Front. Physiol. 11, 542950.
Hayashi, T., Asano, Y., Shintani, Y., Aoyama, H., Kioka, H., Tsukamoto, O., Hikita, M., Shinzawa-Itoh, K., Takafuji, K., Higo, S., Kato, H., Yamazaki, S., Matsuoka, K., Nakano, A., Asanuma, H., Asakura, M., Minamino, T., Goto, Y., Ogura, T., Kitakaze, M., Komuro, I., Sakata, Y., Tsukihara, T., Yoshikawa, S., Takashima, S., 2015. Higd1a is a positive regulator of cytochrome c oxidase. Proc. Natl. Acad. Sci. U. S. A. 112 (5), 1553–1558.
Helassa, N., Durst, C.D., Coates, C., Kerruth, S., Arif, U., Schulze, C., Wiegert, J.S., Geeves, M., Oertner, T.G., Torok, K., 2018. Ultrafast glutamate sensors resolve high-frequency release at Schaffer collateral synapses. Proc. Natl. Acad. Sci. U. S. A. 115 (21), 5594–5599.
Hellweg, L., Edenhofer, A., Barck, L., Huppertz, M.C., Frei, M.S., Tarnawski, M., Bergner, A., Koch, B., Johnsson, K., Hiblot, J., 2023. A general method for the development of multicolor biosensors with large dynamic ranges. Nat. Chem. Biol. 19 (9), 1147–1157.
Helman, G., Pacheco-Colon, I., Gropman, A.L., 2014. The urea cycle disorders. Semin. Neurol. 34 (3), 341–349.
Herzig, S., Raemy, E., Montessuit, S., Veuthey, J.L., Zamboni, N., Westermann, B., Kunji, E.R., Martinou, J.C., 2012. Identification and functional expression of the mitochondrial pyruvate carrier. Science 337 (6090), 93–96.
Ho, L., Wexler, I.D., Liu, T.C., Thekkumkara, T.J., Patel, M.S., 1989. Characterization of cDNAs encoding human pyruvate dehydrogenase alpha subunit. Proc. Natl. Acad. Sci. U. S. A. 86 (14), 5330–5334.
Horwich, A.L., Kalousek, F., Fenton, W.A., Pollock, R.A., Rosenberg, L.E., 1986. Targeting of pre-ornithine transcarbamylase to mitochondria: definition of critical regions and residues in the leader peptide. Cell 44 (3), 451–459.
Hoyland, L.E., VanLinden, M.R., Niere, M., Stromland, O., Sharma, S., Dietze, J., Tolas, I., Lucena, E., Bifulco, E., Sverkeli, L.J., Cimadamore-Werthein, C., Ashrafi, H., Haukanes, K.F., van der Hoeven, B., Dolle, C., Davidsen, C., Pettersen, I.K.N., Tronstad, K.J., Mjos, S.A., Hayat, F., Makarov, M.V., Migaud, M.E., Heiland, I., Ziegler, M., 2024. Subcellular NAD(+) pools are interconnected and buffered by mitochondrial NAD( ). Nat. Metab. 6 (12), 2319–2337.
Hu, H., Gu, Y., Xu, L., Zou, Y., Wang, A., Tao, R., Chen, X., Zhao, Y., Yang, Y., 2017. A genetically encoded toolkit for tracking live-cell histidine dynamics in space and time. Sci. Rep. 7, 43479.
Hu, J., Dong, L., Outten, C.E., 2008. The redox environment in the mitochondrial intermembrane space is maintained separately from the cytosol and matrix. J. Biol. Chem. 283 (43), 29126–29134.
Hu, Q., Wu, D., Walker, M., Wang, P., Tian, R., Wang, W., 2021. Genetically encoded biosensors for evaluating NAD(+)/NADH ratio in cytosolic and mitochondrial compartments. Cell Rep. Methods 1 (7).
Hui, S., Ghergurovich, J.M., Morscher, R.J., Jang, C., Teng, X., Lu, W., Esparza, L.A., Reya, T., Le, Z., Yanxiang Guo, J., White, E., Rabinowitz, J.D., 2017. Glucose feeds the TCA cycle via circulating lactate. Nature 551 (7678), 115–118.
Hung, Y.P., Albeck, J.G., Tantama, M., Yellen, G., 2011. Imaging cytosolic NADH-NAD(+) redox state with a genetically encoded fluorescent biosensor. Cell Metab. 14 (4), 545–554.
Imamura, H., Nhat, K.P., Togawa, H., Saito, K., Iino, R., Kato-Yamada, Y., Nagai, T., Noji, H., 2009. Visualization of ATP levels inside single living cells with fluorescence resonance energy transfer-based genetically encoded indicators. Proc. Natl. Acad. Sci. U. S. A. 106 (37), 15651–15656.
J, O.U., Jhun, B.S., Hurst, S., Bisetto, S., Gross, P., Chen, M., Kettlewell, S., Park, J., Oyamada, H., Smith, G.L., Murayama, T., Sheu, S.S., 2013. Overexpression of ryanodine receptor type 1 enhances mitochondrial fragmentation and Ca2+-induced ATP production in cardiac H9c2 myoblasts. Am. J. Physiol. Heart Circ. Physiol. 305 (12), H1736–H1751.
Jia, N., Ganesan, D., Guan, H., Jeong, Y.Y., Han, S., Nissenbaum, M., Kusnecov, A.W., Cai, Q., 2024. Mitochondrial bioenergetics stimulates autophagy for pathological tau clearance in tauopathy neurons. bioRxiv.
Juel, C., Halestrap, A.P., 1999. Lactate transport in skeletal muscle - role and regulation of the monocarboxylate transporter. J. Physiol. 517 (Pt 3), 633–642. Pt 3.
Kamikubo, K., Kato, H., Kioka, H., Yamazaki, S., Tsukamoto, O., Nishida, Y., Asano, Y., Imamura, H., Kawahara, H., Shintani, Y., Takashima, S., 2019. A molecular triage process mediated by RING finger protein 126 and BCL2-associated athanogene 6 regulates degradation of G(0)/G(1) switch gene 2. J. Biol. Chem. 294 (40), 14562–14573.
Kanazawa, M., Yano, M., Namchai, C., Yamamoto, S., Ohtake, A., Takayanagi, M., Mori, M., Niimi, H., 1997. Visualization of mitochondria with green fluorescent protein in cultured fibroblasts from patients with mitochondrial diseases. Biochem. Biophys. Res. Commun. 239 (2), 580–584.
Kealey, J., Dussmann, H., Llorente-Folch, I., Niewidok, N., Salvucci, M., Prehn, J.H.M., D'Orsi, B., 2022. Effect of TP53 deficiency and KRAS signaling on the bioenergetics of colon cancer cells in response to different substrates: a single cell study. Front. Cell Dev. Biol. 10, 893677.
Kennedy, B.E., Madreiter, C.T., Vishnu, N., Malli, R., Graier, W.F., Karten, B., 2014. Adaptations of energy metabolism associated with increased levels of mitochondrial cholesterol in Niemann-Pick type C1-deficient cells. J. Biol. Chem. 289 (23), 16278–16289.
Kennedy, E.P., Lehninger, A.L., 1949. Oxidation of fatty acids and tricarboxylic acid cycle intermediates by isolated rat liver mitochondria. J. Biol. Chem. 179 (2), 957–972.

Kioka, H., Kato, H., Fujikawa, M., Tsukamoto, O., Suzuki, T., Imamura, H., Nakano, A., Higo, S., Yamazaki, S., Matsuzaki, T., Takafuji, K., Asanuma, H., Asakura, M., Minamino, T., Shintani, Y., Yoshida, M., Noji, H., Kitakaze, M., Komuro, I., Asano, Y., Takashima, S., 2014. Evaluation of intramitochondrial ATP levels identifies G0/G1 switch gene 2 as a positive regulator of oxidative phosphorylation. Proc. Natl. Acad. Sci. U. S. A. 111 (1), 273–278.

Kioka, H., Kato, H., Fujita, T., Asano, Y., Shintani, Y., Yamazaki, S., Tsukamoto, O., Imamura, H., Kogo, M., Kitakaze, M., Sakata, Y., Takashima, S., 2020. In vivo real-time ATP imaging in zebrafish hearts reveals G0s2 induces ischemic tolerance. FASEB J. 34 (2), 2041–2054.

Kong, B.W., Kim, H., Foster, D.N., 2003. Expression analysis and mitochondrial targeting properties of the chicken manganese-containing superoxide dismutase. Biochim. Biophys. Acta 1625 (1), 98–108.

Koshenov, Z., Oflaz, F.E., Hirtl, M., Gottschalk, B., Rost, R., Malli, R., Graier, W.F., 2022. Citrin mediated metabolic rewiring in response to altered basal subcellular Ca(2+) homeostasis. Commun. Biol. 5 (1), 76.

Koshenov, Z., Oflaz, F.E., Hirtl, M., Pilic, J., Bachkoenig, O.A., Gottschalk, B., Madreiter-Sokolowski, C.T., Rost, R., Malli, R., Graier, W.F., 2021. Sigma-1 receptor promotes mitochondrial bioenergetics by orchestrating ER Ca(2+) leak during early ER stress. Metabolites 11 (7).

Koveal, D., Rosen, P.C., Meyer, D.J., Diaz-Garcia, C.M., Wang, Y., Cai, L.H., Chou, P.J., Weitz, D.A., Yellen, G., 2022. A high-throughput multiparameter screen for accelerated development and optimization of soluble genetically encoded fluorescent biosensors. Nat. Commun. 13 (1), 2919.

Krebs, H.A., Johnson, W.A., 1980. The role of citric acid in intermediate metabolism in animal tissues. FEBS Lett. 117 (Suppl. l), K1–K10.

Krebs, H.A.a., J, W.A., 1937. The role of citric acid in intermediate metabolism in animal tissues. Enzymologia 4, 148–151.

Lauterboeck, L., Kang, S.W., White 3rd, D., Bao, R., Mobasheran, P., Yang, Q., 2024. IF1 promotes cellular proliferation and inhibits oxidative phosphorylation in Mouse embryonic fibroblasts under normoxia and hypoxia. Cells 13 (6).

Lee, S., Park, D., Lim, C., Kim, J.-I., Min, K.-T., 2022. mtIF3 is locally translated in axons and regulates mitochondrial translation for axonal growth. BMC Biol. 20 (1), 12.

Lee, S., Wang, W., Hwang, J., Namgung, U., Min, K.T., 2019. Increased ER-mitochondria tethering promotes axon regeneration. Proc. Natl. Acad. Sci. U. S. A. 116 (32), 16074–16079.

Lefkimmiatis, K., Leronni, D., Hofer, A.M., 2013. The inner and outer compartments of mitochondria are sites of distinct cAMP/PKA signaling dynamics. J. Cell Biol. 202 (3), 453–462.

Lehninger, A.L., 1946. A quantitative study of the products of fatty acid oxidation in liver suspensions. J. Biol. Chem. 164, 291–306.

Leung, H.H., Mansour, C., Rousseau, M., Nakhla, A., Kiselyov, K., Venkatachalam, K., Wong, C.O., 2024. Drosophila tweety facilitates autophagy to regulate mitochondrial homeostasis and bioenergetics in glia. Glia 72 (2), 433–451.

Li, L., Cheng, Y., Shen, S., Zhou, J., Wang, A., Chen, G., Xu, J., Yang, Y., Zhao, Y., Zhang, S., Tian, Y., 2020. Sensitive detection via the time-resolved fluorescence of circularly permuted yellow fluorescent protein biosensors. Sensor. Actuator. B Chem. 321, 128614.

Li, X., Zhang, Y., Xu, L., Wang, A., Zou, Y., Li, T., Huang, L., Chen, W., Liu, S., Jiang, K., Zhang, X., Wang, D., Zhang, L., Zhang, Z., Zhang, Z., Chen, X., Jia, W., Zhao, A., Yan, X., Zhou, H., Zhu, L., Ma, X., Ju, Z., Jia, W., Wang, C., Loscalzo, J., Yang, Y., Zhao, Y., 2023. Ultrasensitive sensors reveal the spatiotemporal landscape of lactate metabolism in physiology and disease. Cell Metab. 35 (1), 200–211 e209.

Liu, A., Huang, X., He, W., Xue, F., Yang, Y., Liu, J., Chen, L., Yuan, L., Xu, P., 2021. pHmScarlet is a pH-sensitive red fluorescent protein to monitor exocytosis docking and fusion steps. Nat. Commun. 12 (1), 1413.

Liu, B., Zhao, Z., Wang, P., Aihemaiti, K., Zhu, L., Wei, Q., Li, W., Yuan, X., Wu, J., Jiang, C., Hao, M., Wang, J., 2025. GlutaR: a high-performance fluorescent protein-based sensor for spatiotemporal monitoring of glutamine dynamics in vivo. Angew Chem. Int. Ed. Engl. 64 (4), e202416608.

Liu, X., Kim, C.N., Yang, J., Jemmerson, R., Wang, X., 1996. Induction of apoptotic program in cell-free extracts: requirement for dATP and cytochrome c. Cell 86 (1), 147–157.

Lu, M.-J., Busquets, J., Impedovo, V., Chang, Y.-T., Matsui, W., Tiziani, S., Cambronne, X. A., 2022. SLC25A51 impacts drug sensitivity in AML cells by sustaining mitochondrial oxidative flux. bioRxiv, 2022.2011.2015.516643.

Lucantoni, F., Dussmann, H., Llorente-Folch, I., Prehn, J.H.M., 2018a. BCL2 and BCL(X)L selective inhibitors decrease mitochondrial ATP production in breast cancer cells and are synthetically lethal when combined with 2-deoxy-D-glucose. Oncotarget 9 (40), 26046–26063.

Lucantoni, F., Dussmann, H., Prehn, J.H.M., 2018b. Metabolic targeting of breast cancer cells with the 2-Deoxy-D-Glucose and the mitochondrial Bioenergetics inhibitor MDIVI-1. Front. Cell Dev. Biol. 6, 113.

Lucantoni, F., Salvucci, M., Dussmann, H., Lindner, A.U., Lambrechts, D., Prehn, J.H.M., 2021. BCL(X)L and BCL2 increase the metabolic fitness of breast cancer cells: a single-cell imaging study. Cell Death Differ. 28 (5), 1512–1531.

Ludtmann, M.H., Angelova, P.R., Ninkina, N.N., Gandhi, S., Buchman, V.L., Abramov, A. Y., 2016. Monomeric Alpha-Synuclein exerts a physiological role on brain ATP synthase. J. Neurosci. 36 (41), 10510–10521.

Ludtmann, M.H.R., Arber, C., Bartolome, F., de Vicente, M., Preza, E., Carro, E., Houlden, H., Gandhi, S., Wray, S., Abramov, A.Y., 2017. Mutations in valosin-containing protein (VCP) decrease ADP/ATP translocation across the mitochondrial membrane and impair energy metabolism in human neurons. J. Biol. Chem. 292 (21), 8907–8917.

Luongo, T.S., Eller, J.M., Lu, M.J., Niere, M., Raith, F., Perry, C., Bornstein, M.R., Oliphint, P., Wang, L., McReynolds, M.R., Migaud, M.E., Rabinowitz, J.D., Johnson, F.B., Johnsson, K., Ziegler, M., Cambronne, X.A., Baur, J.A., 2020. SLC25A51 is a mammalian mitochondrial NAD(+) transporter. Nature 588 (7836), 174–179.

Lynch, E.M., Hansen, H., Salay, L., Cooper, M., Timr, S., Kollman, J.M., Webb, B.A., 2024. Structural basis for allosteric regulation of human phosphofructokinase-1. Nat. Commun. 15 (1), 7323.

MacDonald, J.A., Bothun, A.M., Annis, S.N., Sheehan, H., Ray, S., Gao, Y., Ivanov, A.R., Khrapko, K., Tilly, J.L., Woods, D.C., 2019. A nanoscale, multi-parametric flow cytometry-based platform to study mitochondrial heterogeneity and mitochondrial DNA dynamics. Commun. Biol. 2, 258.

Madaris, T.R., Venkatesan, M., Maity, S., Stein, M.C., Vishnu, N., Venkateswaran, M.K., Davis, J.G., Ramachandran, K., Uthayabalan, S., Allen, C., Osidele, A., Stanley, K., Bigham, N.P., Bakewell, T.M., Narkunan, M., Le, A., Karanam, V., Li, K., Mhapankar, A., Norton, L., Ross, J., Aslam, M.I., Reeves, W.B., Singh, B.B., Caplan, J., Wilson, J.J., Stathopulos, P.B., Baur, J.A., Madesh, M., 2023. Limiting Mrs2-dependent mitochondrial Mg(2+) uptake induces metabolic programming in prolonged dietary stress. Cell Rep. 42 (3), 112155.

Madreiter-Sokolowski, C.T., Gottschalk, B., Parichatikanond, W., Eroglu, E., Klec, C., Waldeck-Weiermair, M., Malli, R., Graier, W.F., 2016. Resveratrol specifically kills cancer cells by a devastating increase in the Ca2+ coupling between the greatly tethered endoplasmic reticulum and Mitochondria. Cell. Physiol. Biochem. 39 (4), 1404–1420.

Martinez-Reyes, I., Chandel, N.S., 2020. Mitochondrial TCA cycle metabolites control physiology and disease. Nat. Commun. 11 (1), 102.

Marvin, J.S., Kokotos, A.C., Kumar, M., Pulido, C., Tkachuk, A.N., Yao, J.S., Brown, T.A., Ryan, T.A., 2024. iATPSnFR2: a high-dynamic-range fluorescent sensor for monitoring intracellular ATP. Proc. Natl. Acad. Sci. U. S. A. 121 (21), e2314604121.

Matsuda, N., Hironaka, K.-i., Fujii, M., Wada, T., Kunida, K., Inoue, H., Eto, M., Hoshino, D., Furuichi, Y., Manabe, Y., Fujii, N.L., Noji, H., Imamura, H., Kuroda, S., 2020. Monitoring and mathematical modeling of mitochondrial ATP in myotubes at single-cell level reveals two distinct population with different kinetics. Quant. Biol. 8 (3), 228–237.

McBride, H.M., Neuspiel, M., Wasiak, S., 2006. Mitochondria: more than just a powerhouse. Curr. Biol. 16 (14), R551–R560.

Miyawaki, A., Llopis, J., Heim, R., McCaffery, J.M., Adams, J.A., Ikura, M., Tsien, R.Y., 1997. Fluorescent indicators for Ca2+ based on green fluorescent proteins and calmodulin. Nature 388 (6645), 882–887.

Molinari, P.E., Krapp, A.R., Weiner, A., Beyer, H.M., Kondadi, A.K., Blomeier, T., Lopez, M., Bustos-Sanmamed, P., Tevere, E., Weber, W., Reichert, A.S., Calcaterra, N. B., Beller, M., Carrillo, N., Zurbriggen, M.D., 2023. NERNST: a genetically-encoded ratiometric non-destructive sensing tool to estimate NADP(H) redox status in bacterial, plant and animal systems. Nat. Commun. 14 (1), 3277.

Moon, S.J., Chiappino-Pepe, A., Dong, W., Kelleher, J.K., Vander Heiden, M., Stephanopoulos, G., Sikes, H.D., 2024. NADPH composite index analysis quantifies the relationship between compartmentalized NADPH dynamics and growth rates in cancer cells. bioRxiv.

Moon, S.J., Dong, W., Stephanopoulos, G.N., Sikes, H.D., 2020. Oxidative pentose phosphate pathway and glucose anaplerosis support maintenance of mitochondrial NADPH pool under mitochondrial oxidative stress. Bioeng. Transl. Med. 5 (3), e10184.

Murata, M.M., Kong, X., Moncada, E., Chen, Y., Imamura, H., Wang, P., Berns, M.W., Yokomori, K., Digman, M.A., 2019. NAD+ consumption by PARP1 in response to DNA damage triggers metabolic shift critical for damaged cell survival. Mol. Biol. Cell 30 (20), 2584–2597.

N'Gadjaga, M.D., Perrinet, S., Connor, M.G., Bertolin, G., Millot, G.A., Subtil, A., 2022. Chlamydia trachomatis development requires both host glycolysis and oxidative phosphorylation but has only minor effects on these pathways. J. Biol. Chem. 298 (9), 102338.

Nagai, H., Satomi, T., Abiru, A., Miyamoto, K., Nagasawa, K., Maruyama, M., Yamamoto, S., Kikuchi, K., Fuse, H., Noda, M., Tsujihata, Y., 2017. Antihypertrophic effects of small molecules that maintain mitochondrial ATP levels under hypoxia. EBioMedicine 24, 147–158.

Nagao, T., Shintani, Y., Hayashi, T., Kioka, H., Kato, H., Nishida, Y., Yamazaki, S., Tsukamoto, O., Yashirogi, S., Yazawa, I., Asano, Y., Shinzawa-Itoh, K., Imamura, H., Suzuki, T., Suzuki, T., Goto, Y.I., Takashima, S., 2020. Higd1a improves respiratory function in the models of mitochondrial disorder. FASEB J. 34 (1), 1859–1871.

Nakamura, H., Rho, E., Lee, C.T., Itoh, K., Deng, D., Watanabe, S., Razavi, S., Matsubayashi, H.T., Zhu, C., Jung, E., Rangamani, P., Watanabe, S., Inoue, T., 2023. ActuAtor, a Listeria-inspired molecular tool for physical manipulation of intracellular organizations through de novo actin polymerization. Cell Rep. 42 (10), 113089.

Nakano, M., Imamura, H., Nagai, T., Noji, H., 2011. Ca(2)(+) regulation of mitochondrial ATP synthesis visualized at the single cell level. ACS Chem. Biol. 6 (7), 709–715.

Nakano, M., Imamura, H., Sasaoka, N., Yamamoto, M., Uemura, N., Shudo, T., Fuchigami, T., Takahashi, R., Kakizuka, A., 2017. ATP maintenance via two types of ATP regulators mitigates pathological phenotypes in mouse models of Parkinson's disease. EBioMedicine 22, 225–241.

Nasu, Y., Aggarwal, A., Le, G.N.T., Vo, C.T., Kambe, Y., Wang, X., Beinlich, F.R.M., Lee, A.B., Ram, T.R., Wang, F., Gorzo, K.A., Kamijo, Y., Boisvert, M., Nishinami, S., Kawamura, G., Ozawa, T., Toda, H., Gordon, G.R., Ge, S., Hirase, H., Nedergaard, M., Paquet, M.E., Drobizhev, M., Podgorski, K., Campbell, R.E., 2023. Lactate biosensors for spectrally and spatially multiplexed fluorescence imaging. Nat. Commun. 14 (1), 6598.

Neary, M.T., Ng, K.E., Ludtmann, M.H., Hall, A.R., Piotrowska, I., Ong, S.B., Hausenloy, D.J., Mohun, T.J., Abramov, A.Y., Breckenridge, R.A., 2014. Hypoxia

signaling controls postnatal changes in cardiac mitochondrial morphology and function. J. Mol. Cell. Cardiol. 74 (100), 340–352.
Nerlich, A., Mieth, M., Letsiou, E., Fatykhova, D., Zscheppang, K., Imai-Matsushima, A., Meyer, T.F., Paasch, L., Mitchell, T.J., Tonnies, M., Bauer, T.T., Schneider, P., Neudecker, J., Ruckert, J.C., Eggeling, S., Schimek, M., Witzenrath, M., Suttorp, N., Hippenstiel, S., Hocke, A.C., 2018. Pneumolysin induced mitochondrial dysfunction leads to release of mitochondrial DNA. Sci. Rep. 8 (1), 182.
Nunnari, J., Suomalainen, A., 2012. Mitochondria: in sickness and in health. Cell 148 (6), 1145–1159.
Oflaz, F.E., Koshenov, Z., Hirtl, M., Rost, R., Malli, R., Graier, W.F., 2022. Sigma-1 receptor modulation by ligands coordinates cancer cell energy metabolism. Biomolecules 12 (6).
Owen, O.E., Kalhan, S.C., Hanson, R.W., 2002. The key role of anaplerosis and cataplerosis for citric acid cycle function. J. Biol. Chem. 277 (34), 30409–30412.
Owen, R.I., Lewin, A.P., Peel, A., Wang, J., Guy, J., Hauswirth, W.W., Stacpoole, P.W., Flotte, T.R., 2000. Recombinant adeno-associated virus vector-based gene transfer for defects in oxidative metabolism. Hum. Gene Ther. 11 (15), 2067–2078.
Passonneau, J.V., Lowry, O.H., 1964. The role of phosphofructokinase in metabolic regulation. Adv. Enzym. Regul. 2, 265–274.
Patel, M.S., Korotchkina, L.G., 2006. Regulation of the pyruvate dehydrogenase complex. Biochem. Soc. Trans. 34 (Pt 2), 217–222.
Pavlyuchenkova, A.N., Zinovkin, R.A., Makievskaya, C.I., Galkin, I.I., Chelombitko, M.A., 2022. Mitochondria-targeted triphenylphosphonium-based compounds inhibit FcεRI-dependent degranulation of mast cells by preventing mitochondrial dysfunction through Erk1/2. Life Sci. 288, 120174.
Pilic, J., Gottschalk, B., Bourgeois, B., Habisch, H., Koshenov, Z., Oflaz, F.E., Erdogan, Y. C., Miri, S.M., Yigit, E.N., Aydin, M.S., Ozturk, G., Eroglu, E., Shoshan-Barmatz, V., Madl, T., Graier, W.F., Malli, R., 2024. Hexokinase 1 forms rings that regulate mitochondrial fission during energy stress. Mol. Cells 84 (14), 2732–2746 e2735.
Plecita-Hlavata, L., Engstova, H., Holendova, B., Tauber, J., Spacek, T., Petraskova, L., Kren, V., Spackova, J., Gotvaldova, K., Jezek, J., Dlaskova, A., Smolkova, K., Jezek, P., 2020. Mitochondrial superoxide production decreases on glucose-stimulated insulin secretion in pancreatic beta cells due to decreasing mitochondrial matrix NADH/NAD(+) ratio. Antioxidants Redox Signal. 33 (12), 789–815.
Poburko, D., Santo-Domingo, J., Demaurex, N., 2011. Dynamic regulation of the mitochondrial proton gradient during cytosolic calcium elevations. J. Biol. Chem. 286 (13), 11672–11684.
Poorman, R.A., Randolph, A., Kemp, R.G., Heinrikson, R.L., 1984. Evolution of phosphofructokinase–gene duplication and creation of new effector sites. Nature 309 (5967), 467–469.
Quintana-Cabrera, R., Manjarres-Raza, I., Vicente-Gutierrez, C., Corrado, M., Bolanos, J. P., Scorrano, L., 2021. Opa1 relies on cristae preservation and ATP synthase to curtail reactive oxygen species accumulation in mitochondria. Redox Biol. 41, 101944.
Quintana-Cabrera, R., Quirin, C., Glytsou, C., Corrado, M., Urbani, A., Pellattiero, A., Calvo, E., Vazquez, J., Enriquez, J.A., Gerle, C., Soriano, M.E., Bernardi, P., Scorrano, L., 2018. The cristae modulator optic atrophy 1 requires mitochondrial ATP synthase oligomers to safeguard mitochondrial function. Nat. Commun. 9 (1), 3399.
Rauseo, D., Contreras-Baeza, Y., Faurand, H., Carcamo, N., Suarez, R., von Faber-Castell, A., Silva, F., Mora-Gonzalez, V., Wyss, M.T., Baeza-Lehnert, F., Ruminot, I., Alvarez-Navarro, C., San Martin, A., Weber, B., Sandoval, P.Y., Barros, L.F., 2024. Lactate-carried mitochondrial energy overflow. bioRxiv.
Rauter, T., Burgstaller, S., Gottschalk, B., Ramadani-Muja, J., Bischof, H., Hay, J.C., Graier, W.F., Malli, R., 2020a. ER-to-Golgi transport in HeLa cells displays high resilience to Ca(2+) and energy stresses. Cells 9 (10).
Rauter, T., Depaoli, M.R., Bischof, H., Graier, W.F., Malli, R., 2020b. Metabolic profiling of single cancer cells using mitochondrial ATP probes. STAR Protoc 1 (2), 100048.
Richetin, K., Steullet, P., Pachoud, M., Perbet, R., Parietti, E., Maheswaran, M., Eddarkaoui, S., Begard, S., Pythoud, C., Rey, M., Caillierez, R., K, Q.D., Halliez, S., Bezzi, P., Buee, L., Leuba, G., Colin, M., Toni, N., Deglon, N., 2020. Tau accumulation in astrocytes of the dentate gyrus induces neuronal dysfunction and memory deficits in Alzheimer's disease. Nat. Neurosci. 23 (12), 1567–1579.
Rizzo, M.A., Springer, G.H., Granada, B., Piston, D.W., 2004. An improved cyan fluorescent protein variant useful for FRET. Nat. Biotechnol. 22 (4), 445–449.
Rizzuto, R., Brini, M., Pizzo, P., Murgia, M., Pozzan, T., 1995. Chimeric green fluorescent protein as a tool for visualizing subcellular organelles in living cells. Curr. Biol. 5 (6), 635–642.
Rojo, E.E., Stuart, R.A., Neupert, W., 1995. Conservative sorting of F0-ATPase subunit 9: export from matrix requires delta pH across inner membrane and matrix ATP. EMBO J. 14 (14), 3445–3451.
Rossi, A., Rigotto, G., Valente, G., Giorgio, V., Basso, E., Filadi, R., Pizzo, P., 2020. Defective mitochondrial pyruvate flux affects cell bioenergetics in alzheimer's disease-related models. Cell Rep. 30 (7), 2332–2348 e2310.
Rueda, C.B., Traba, J., Amigo, I., Llorente-Folch, I., Gonzalez-Sanchez, P., Pardo, B., Esteban, J.A., del Arco, A., Satrustegui, J., 2015. Mitochondrial ATP-Mg/Pi carrier SCaMC-3/Slc25a23 counteracts PARP-1-dependent fall in mitochondrial ATP caused by excitotoxic insults in neurons. J. Neurosci. 35 (8), 3566–3581.
Sahan, A.Z., Youngblood, E., Das, S., Schmitt, D.L., Zhang, J., 2023. An expanded palette of ATP sensors for subcellular and multiplexed imaging. bioRxiv, 2023.2005.2001.538722.
San Martin, A., Arce-Molina, R., Aburto, C., Baeza-Lehnert, F., Barros, L.F., Contreras-Baeza, Y., Pinilla, A., Ruminot, I., Rauseo, D., Sandoval, P.Y., 2022. Visualizing physiological parameters in cells and tissues using genetically encoded indicators for metabolites. Free Radic. Biol. Med. 182, 34–58.
Sano, S., Inoue, S., Tanabe, Y., Sumiya, C., Koike, S., 1959. Significance of mitochondria for porphyrin and heme biosynthesis. Science 129 (3344), 275–276.
Satoh, A.O., Fujioka, Y., Kashiwagi, S., Yoshida, A., Fujioka, M., Sasajima, H., Nanbo, A., Amano, M., Ohba, Y., 2023. Interaction between PI3K and the VDAC2 channel tethers Ras-PI3K-positive endosomes to mitochondria and promotes endosome maturation. Cell Rep. 42 (3), 112229.
Shibata, T., Yamashita, S., Hirusaki, K., Katoh, K., Ohta, Y., 2015. Isolation of mitochondria by gentle cell membrane disruption, and their subsequent characterization. Biochem. Biophys. Res. Commun. 463 (4), 563–568.
Shindo, Y., Komatsu, H., Hotta, K., Ariga, K., Oka, K., 2016. An artificial reaction promoter modulates mitochondrial functions via chemically promoting protein acetylation. Sci. Rep. 6, 29224.
Shinoda, H., Ma, Y., Nakashima, R., Sakurai, K., Matsuda, T., Nagai, T., 2018. Acid-Tolerant monomeric GFP from Olindias formosa. Cell Chem. Biol. 25 (3), 330–338 e337.
Shintani, Y., Drexler, H.C., Kioka, H., Terracciano, C.M., Coppen, S.R., Imamura, H., Akao, M., Nakai, J., Wheeler, A.P., Higo, S., Nakayama, H., Takashima, S., Yashiro, K., Suzuki, K., 2014. Toll-like receptor 9 protects non-immune cells from stress by modulating mitochondrial ATP synthesis through the inhibition of SERCA2. EMBO Rep. 15 (4), 438–445.
Singh, G., George, G., Raja, S.O., Kandaswamy, P., Kumar, M., Thutupalli, S., Laxman, S., Gulyani, A., 2023. A molecular rotor FLIM probe reveals dynamic coupling between mitochondrial inner membrane fluidity and cellular respiration. Proc. Natl. Acad. Sci. U. S. A. 120 (24), e2213241120.
Smith, J.J., Valentino, T.R., Ablicki, A.H., Banerjee, R., Colligan, A.R., Eckert, D.M., Desjardins, G.A., Diehl, K.L., 2024. A genetically-encoded fluorescent biosensor for visualization of acetyl-CoA in live cells. bioRxiv.
Smith, K.R., Hayat, F., Andrews, J.F., Migaud, M.E., Gassman, N.R., 2019. Dihydroxyacetone exposure alters NAD(P)H and induces mitochondrial stress and autophagy in HEK293T cells. Chem. Res. Toxicol. 32 (8), 1722–1731.
Spurlock, B., Gupta, P., Basu, M.K., Mukherjee, A., Hjelmeland, A.B., Darley-Usmar, V., Parker, D., Foxall, M.E., Mitra, K., 2019. New quantitative approach reveals heterogeneity in mitochondrial structure-function relations in tumor-initiating cells. J Cell Sci 132 (9).
Spurlock, B., Mitra, K., 2021. Mito-SinCe(2) approach to analyze mitochondrial structure-function relationship in single cells. Methods Mol. Biol. 2275, 415–432.
Sullivan, L.B., Gui, D.Y., Hosios, A.M., Bush, L.N., Freinkman, E., Vander Heiden, M.G., 2015. Supporting aspartate biosynthesis is an essential function of respiration in proliferating cells. Cell 162 (3), 552–563.
Suzuki, R., Hotta, K., Oka, K., 2018. Transitional correlation between inner-membrane potential and ATP levels of neuronal mitochondria. Sci. Rep. 8 (1), 2993.
Tanaka, T., Nagashima, K., Inagaki, N., Kioka, H., Takashima, S., Fukuoka, H., Noji, H., Kakizuka, A., Imamura, H., 2014. Glucose-stimulated single pancreatic islets sustain increased cytosolic ATP levels during initial Ca2+ influx and subsequent Ca2+ oscillations. J. Biol. Chem. 289 (4), 2205–2216.
Tantama, M., Martinez-Francois, J.R., Mongeon, R., Yellen, G., 2013. Imaging energy status in live cells with a fluorescent biosensor of the intracellular ATP-to-ADP ratio. Nat. Commun. 4, 2550.
Tao, R., Zhao, Y., Chu, H., Wang, A., Zhu, J., Chen, X., Zou, Y., Shi, M., Liu, R., Su, N., Du, J., Zhou, H.M., Zhu, L., Qian, X., Liu, H., Loscalzo, J., Yang, Y., 2017. Genetically encoded fluorescent sensors reveal dynamic regulation of NADPH metabolism. Nat. Methods 14 (7), 720–728.
Thornton, K., Wang, Y., Weiner, H., Gorenstein, D.G., 1993. Import, processing, and two-dimensional NMR structure of a linker-deleted signal peptide of rat liver mitochondrial aldehyde dehydrogenase. J. Biol. Chem. 268 (26), 19906–19914.
Tiwari, A., Myeong, J., Hashemiaghdam, A., Zhang, H., Niu, X., Laramie, M.A., Stunault, M.I., Sponagel, J., Patti, G., Shriver, L., Klyachko, V., Ashrafi, G., 2024. Mitochondrial pyruvate transport regulates presynaptic metabolism and neurotransmission. bioRxiv.
Tkatch, T., Greotti, E., Baranauskas, G., Pendin, D., Roy, S., Nita, L.I., Wettmarshausen, J., Prigge, M., Yizhar, O., Shirihai, O.S., Fishman, D., Hershfinkel, M., Fleidervish, I.A., Perocchi, F., Pozzan, T., Sekler, I., 2017. Optogenetic control of mitochondrial metabolism and Ca(2+) signaling by mitochondria-targeted opsins. Proc. Natl. Acad. Sci. U. S. A. 114 (26), E5167–E5176.
Trinh, A.L., Ber, S., Howitt, A., Valls, P.O., Fries, M.W., Venkitaraman, A.R., Esposito, A., 2019. Fast single-cell biochemistry: theory, open source microscopy and applications. Methods Appl. Fluoresc. 7 (4), 044001.
Tsuno, S., Harada, K., Horikoshi, M., Mita, M., Kitaguchi, T., Hirai, M.Y., Matsumoto, M., Tsuboi, T., 2024. Mitochondrial ATP concentration decreases immediately after glucose administration to glucose-deprived hepatocytes. FEBS Open Bio 14 (1), 79–95.
van den Boogaart, P., Samallo, J., Agsteribbe, E., 1982. Similar genes for a mitochondrial ATPase subunit in the nuclear and mitochondrial genomes of Neurospora crassa. Nature 298 (5870), 187–189.
van der Stel, W., Yang, H., Vrijenhoek, N.G., Schimming, J.P., Callegaro, G., Carta, G., Darici, S., Delp, J., Forsby, A., White, A., le Devedec, S., Leist, M., Jennings, P., Beltman, J.B., van de Water, B., Danen, E.H.J., 2022. Mapping the cellular response to electron transport chain inhibitors reveals selective signaling networks triggered by mitochondrial perturbation. Arch. Toxicol. 96 (1), 259–285.
van Hameren, G., Campbell, G., Deck, M., Berthelot, J., Chrast, R., Tricaud, N., 2018. CMT disease 2A and demyelination decouple ATP and ROS production by axonal mitochondria. bioRxiv, 462523.
van Hameren, G., Campbell, G., Deck, M., Berthelot, J., Gautier, B., Quintana, P., Chrast, R., Tricaud, N., 2019. In vivo real-time dynamics of ATP and ROS production in axonal mitochondria show decoupling in mouse models of peripheral neuropathies. Acta Neuropathol. Commun. 7 (1), 86.

Vasington, F.D., Murphy, J.V., 1962. Ca ion uptake by rat kidney mitochondria and its dependence on respiration and phosphorylation. J. Biol. Chem. 237, 2670–2677.
Vestweber, D., Schatz, G., 1988. Point mutations destabilizing a precursor protein enhance its post-translational import into mitochondria. EMBO J. 7 (4), 1147–1151.
Vishnu, N., Jadoon Khan, M., Karsten, F., Groschner, L.N., Waldeck-Weiermair, M., Rost, R., Hallstrom, S., Imamura, H., Graier, W.F., Malli, R., 2014. ATP increases within the lumen of the endoplasmic reticulum upon intracellular Ca2+ release. Mol. Biol. Cell 25 (3), 368–379.
von Heijne, G., 1986. Mitochondrial targeting sequences may form amphiphilic helices. EMBO J. 5 (6), 1335–1342.
Waldeck-Weiermair, M., Jean-Quartier, C., Rost, R., Khan, M.J., Vishnu, N., Bondarenko, A.I., Imamura, H., Malli, R., Graier, W.F., 2011. Leucine zipper EF hand-containing transmembrane protein 1 (Letm1) and uncoupling proteins 2 and 3 (UCP2/3) contribute to two distinct mitochondrial Ca2+ uptake pathways. J. Biol. Chem. 286 (32), 28444–28455.
Wang, L., Zhou, X., Lu, T., 2025. Role of mitochondria in physiological activities, diseases, and therapy. Mol. Biomed. 6 (1), 42.
Ward, J.M., Stoyas, C.A., Switonski, P.M., Ichou, F., Fan, W., Collins, B., Wall, C.E., Adanyeguh, I., Niu, C., Sopher, B.L., Kinoshita, C., Morrison, R.S., Durr, A., Muotri, A.R., Evans, R.M., Mochel, F., La Spada, A.R., 2019. Metabolic and Organelle morphology defects in mice and human patients define spinocerebellar ataxia type 7 as a mitochondrial disease. Cell Rep. 26 (5), 1189–1202 e1186.
Watanabe, S., Nihongaki, Y., Itoh, K., Uyama, T., Toda, S., Watanabe, S., Inoue, T., 2022. Defunctionalizing intracellular organelles such as mitochondria and peroxisomes with engineered phospholipase A/acyltransferases. Nat. Commun. 13 (1), 4413.
Weiss-Sadan, T., Ge, M., Hayashi, M., Gohar, M., Yao, C.H., de Groot, A., Harry, S., Carlin, A., Fischer, H., Shi, L., Wei, T.Y., Adelmann, C.H., Wolf, K., Vornbaumen, T., Durr, B.R., Takahashi, M., Richter, M., Zhang, J., Yang, T.Y., Vijay, V., Fisher, D.E., Hata, A.N., Haigis, M.C., Mostoslavsky, R., Bardeesy, N., Papagiannakopoulos, T., Bar-Peled, L., 2023. NRF2 activation induces NADH-reductive stress, providing a metabolic vulnerability in lung cancer. Cell Metab. 35 (3), 487–503 e487.
White 3rd, D., Lauterboeck, L., Mobasheran, P., Kitaguchi, T., Chaanine, A.H., Yang, Q., 2023. Real-time visualization of cytosolic and mitochondrial ATP dynamics in response to metabolic stress in cultured cells. Cells 12 (5).
Wiedemann, N., Pfanner, N., 2017. Mitochondrial machineries for protein import and assembly. Annu. Rev. Biochem. 86, 685–714.
Wilde, B.R., Kaadige, M.R., Guillen, K.P., Butterfield, A., Welm, B.E., Ayer, D.E., 2020. Protein synthesis inhibitors stimulate MondoA transcriptional activity by driving an accumulation of glucose 6-phosphate. Cancer Metabol. 8 (1), 27.
Wilde, B.R., Ye, Z., Lim, T.Y., Ayer, D.E., 2019. Cellular acidosis triggers human MondoA transcriptional activity by driving mitochondrial ATP production. eLife 8.
Wright, R.H., Lioutas, A., Le Dily, F., Soronellas, D., Pohl, A., Bonet, J., Nacht, A.S., Samino, S., Font-Mateu, J., Vicent, G.P., Wierer, M., Trabado, M.A., Schelhorn, C., Carolis, C., Macias, M.J., Yanes, O., Oliva, B., Beato, M., 2016. ADP-ribose-derived nuclear ATP synthesis by NUDIX5 is required for chromatin remodeling. Science 352 (6290), 1221–1225.
Writzl, K., Maver, A., Kovacic, L., Martinez-Valero, P., Contreras, L., Satrustegui, J., Castori, M., Faivre, L., Lapunzina, P., van Kuilenburg, A.B.P., Radovic, S., Thauvin-Robinet, C., Peterlin, B., Del Arco, A., Hennekam, R.C., 2017. De Novo Mutations in SLC25A24 Cause a Disorder Characterized by Early Aging, Bone Dysplasia, Characteristic Face, and Early Demise. Am. J. Hum. Genet. 101 (5), 844–855.
Wu, D., Tan, B., Sun, Y., Hu, Q., 2022. Cystathionine gamma lyase S-sulfhydrates Drp1 to ameliorate heart dysfunction. Redox Biol. 58, 102519.
Xie, T.R., Liu, C.F., Kang, J.S., 2017. Sympathetic transmitters control thermogenic efficacy of brown adipocytes by modulating mitochondrial complex V. Signal Transduct. Targeted Ther. 2, 17060.
Xie, Z., Jones, A., Deeney, J.T., Hur, S.K., Bankaitis, V.A., 2016. Inborn errors of long-chain fatty acid beta-oxidation link neural stem cell self-renewal to autism. Cell Rep. 14 (5), 991–999.
Xue, L., Schnacke, P., Frei, M.S., Koch, B., Hiblot, J., Wombacher, R., Fabritz, S., Johnsson, K., 2023. Probing coenzyme A homeostasis with semisynthetic biosensors. Nat. Chem. Biol. 19 (3), 346–355.
Yamamoto, K., Imamura, H., Ando, J., 2018. Shear stress augments mitochondrial ATP generation that triggers ATP release and Ca(2+) signaling in vascular endothelial cells. Am. J. Physiol. Heart Circ. Physiol. 315 (5), H1477–H1485.
Yamamoto, K., Nogimori, Y., Imamura, H., Ando, J., 2020. Shear stress activates mitochondrial oxidative phosphorylation by reducing plasma membrane cholesterol in vascular endothelial cells. Proc. Natl. Acad. Sci. U. S. A. 117 (52), 33660–33667.
Yamamoto, K., Shimogonya, Y., Maeno, R., Kawabe, K., Ando, J., 2023. Endothelial cells differentially sense laminar and disturbed flows by altering the lipid order of their plasma and mitochondrial membranes. Am. J. Physiol. Cell Physiol. 325 (6), C1532–C1544.
Yong, J., Bischof, H., Burgstaller, S., Siirin, M., Murphy, A., Malli, R., Kaufman, R.J., 2019. Mitochondria supply ATP to the ER through a mechanism antagonized by cytosolic Ca(2). eLife 8.
Yoshida, T., Nakajima, H., Takahashi, S., Kakizuka, A., Imamura, H., 2019. OLIVe: a genetically encoded fluorescent biosensor for quantitative imaging of branched-chain amino acid levels inside single living cells. ACS Sens. 4 (12), 3333–3342.
Zaninello, M., Schlegel, T., Nolte, H., Pirzada, M., Savino, E., Barth, E., Klein, I., Wustenberg, H., Uddin, T., Wolff, L., Wirth, B., Lehmann, H.C., Cioni, J.M., Langer, T., Rugarli, E.I., 2024. CLUH maintains functional mitochondria and translation in motoneuronal axons and prevents peripheral neuropathy. Sci. Adv. 10 (22), eadn2050.
Zhang, M., Wu, J., Sun, R., Tao, X., Wang, X., Kang, Q., Wang, H., Zhang, L., Liu, P., Zhang, J., Xia, Y., Zhao, Y., Yang, Y., Xiong, Y., Guan, K.L., Zou, Y., Ye, D., 2019. SIRT5 deficiency suppresses mitochondrial ATP production and promotes AMPK activation in response to energy stress. PLoS One 14 (2), e0211796.
Zhang, M., Yang, B., Zhang, J., Song, Y., Wang, W., Li, N., Wang, Y., Li, W., Wang, J., 2022. Monitoring the dynamic regulation of the mitochondrial GTP-to-GDP ratio with a genetically encoded fluorescent biosensor. Angew Chem. Int. Ed. Engl. 61 (33), e202201266.
Zhang, S., Ai, H.W., 2020. A general strategy to red-shift green fluorescent protein-based biosensors. Nat. Chem. Biol. 16 (12), 1434–1439.
Zhao, H., Li, T., Wang, K., Zhao, F., Chen, J., Xu, G., Zhao, J., Li, T., Chen, L., Li, L., Xia, Q., Zhou, T., Li, H.Y., Li, A.L., Finkel, T., Zhang, X.M., Pan, X., 2019. AMPK-mediated activation of MCU stimulates mitochondrial Ca(2+) entry to promote mitotic progression. Nat. Cell Biol. 21 (4), 476–486.
Zhao, R., Xu, Y., Wang, X., Zhou, X., Liu, Y., Jiang, S., Zhang, L., Yu, Z., 2022. Withaferin A enhances mitochondrial biogenesis and BNIP3-Mediated mitophagy to promote rapid adaptation to extreme hypoxia. Cells 12 (1).
Zhao, Y., Jin, J., Hu, Q., Zhou, H.M., Yi, J., Yu, Z., Xu, L., Wang, X., Yang, Y., Loscalzo, J., 2011. Genetically encoded fluorescent sensors for intracellular NADH detection. Cell Metab. 14 (4), 555–566.
Zhao, Y., Shen, Y., Wen, Y., Campbell, R.E., 2020. High-performance intensiometric Direct- and inverse-response genetically encoded biosensors for citrate. ACS Cent. Sci. 6 (8), 1441–1450.
Zhao, Y., Takahashi-Yamashiro, K., Shen, Y., Campbell, R.E., 2023. Quantification of intracellular citrate concentrations with genetically encoded biosensors. In: Sharma, M. (Ed.), Fluorescent Proteins: Methods and Protocols. Springer US, New York, NY, pp. 247–258.
Zhao, Y., Yang, Y., 2016. Real-time and high-throughput analysis of mitochondrial metabolic states in living cells using genetically encoded NAD(+)/NADH sensors. Free Radic. Biol. Med. 100, 43–52.
Zhao, Y., Yang, Y., Loscalzo, J., 2014. Real-time assessment of the metabolic profile of living cells with genetically encoded NADH sensors. Methods Enzymol. 542, 349–367.
Zhou, B., Yu, P., Lin, M.Y., Sun, T., Chen, Y., Sheng, Z.H., 2016. Facilitation of axon regeneration by enhancing mitochondrial transport and rescuing energy deficits. J. Cell Biol. 214 (1), 103–119.
Zou, Y., Wang, A., Shi, M., Chen, X., Liu, R., Li, T., Zhang, C., Zhang, Z., Zhu, L., Ju, Z., Loscalzo, J., Yang, Y., Zhao, Y., 2018. Analysis of redox landscapes and dynamics in living cells and in vivo using genetically encoded fluorescent sensors. Nat. Protoc. 13 (10), 2362–2386.